MICROCOP CHART

FOREIGN TECHNOLOGY DIVISION

LASER BASED INFORMATION SYSTEMS

(Selected Pages)

by

L.Z. Kriksunov

DTIC
ELECTE
S JUN 16 1986
D

B

DTIC FILE COPY

HUMAN TRANSLATION

FTD-ID(RS)T-0563-85   22 May 1986

MICROFICHE NR: FTD-86-C-001863

LASER BASED INFORMATION SYSTEMS (Selected Pages)

By: L.Z. Kriksunov

English pages: 134

Source: Sistemy Informatsii s Opticheskimi Kvantovymi
          Generatorami, Publishing House "Tekhnika",
          Kiev, 1970, pp. 124-131; 134-139; 144-147;
          160-229.

Country of origin: USSR
Translated by: SCITRAN
               F33657-84-D-0165
Requester: FTD/SDEO
Approved for public release; Distribution unlimited.

Table of Contents

U. S. BOARD ON GEOGRAPHIC NAMES TRANSLITERATION SYSTEM

Block	Italic	Transliteration	Block	Italic	Transliteration
А а	*А а*	A, a	Р р	*Р р*	R, r
Б б	*Б б*	B, b	С с	*С с*	S, s
В в	*В в*	V, v	Т т	*Т т*	T, t
Г г	*Г г*	G, g	У у	*У у*	U, u
Д д	*Д д*	D, d	Ф ф	*Ф ф*	F, f
Е е	*Е е*	Ye, ye; E, e*	Х х	*Х х*	Kh, kh
Ж ж	*Ж ж*	Zh, zh	Ц ц	*Ц ц*	Ts, ts
З з	*З з*	Z, z	Ч ч	*Ч ч*	Ch, ch
И и	*И и*	I, i	Ш ш	*Ш ш*	Sh, sh
Й й	*Й й*	Y, y	Щ щ	*Щ щ*	Shch, shch
К к	*К к*	K, k	Ъ ъ	*Ъ ъ*	"
Л л	*Л л*	L, l	Ы ы	*Ы ы*	Y, y
М м	*М м*	M, m	Ь ь	*Ь ь*	'
Н н	*Н н*	N, n	Э э	*Э э*	E, e
О о	*О о*	O, o	Ю ю	*Ю ю*	Yu, yu
П п	*П п*	P, p	Я я	*Я я*	Ya, ya

*ye initially, after vowels, and after ъ, ь; e elsewhere.
When written as ё in Russian, transliterate as yё or ё.

RUSSIAN AND ENGLISH TRIGONOMETRIC FUNCTIONS

Russian	English	Russian	English	Russian	English
sin	sin	sh	sinh	arc sh	sinh⁻¹
cos	cos	ch	cosh	arc ch	cosh⁻¹
tg	tan	th	tanh	arc th	tanh⁻¹
ctg	cot	cth	coth	arc cth	coth⁻¹
sec	sec	sch	sech	arc sch	sech⁻¹
cosec	csc	csch	csch	arc csch	csch⁻¹

Russian	English
rot	curl
lg	log

GRAPHICS DISCLAIMER

All figures, graphics, tables, equations, etc. merged into this
translation were extracted from the best quality copy available.

17. METHODS OF INFORMATION RECEPTION

Method of Direct Amplification

The reception system operating in the direct amplification mode consists of the receiving objective, optical filter (decreasing the background radiation), and photoconvertor. The laser radiation used for the transmission of information is amplitude modulated, or consists of consecutive pulses.

The limiting factors of the such systems of direct amplification are the background radiation (causing the respective photocurrent), shot noise, and internal thermal noise of the system.

Signal-to-noise ratio of an optical system with direct amplification and the AM of continuous signal can be calculated by means of the formula [63]

$$n = \frac{\frac{1}{2} m^2 I_c^2 M^2 R_{экв}}{2e\Delta f N M^2 R_{экв} (I_c + I_\phi + I_т) + kT\Delta f},$$ (66)

where m is the coefficient of modulation; I_c and I_ϕ are photocurrents caused by the radiation of the object and the background, respectively; I_t is the current corresponding to the absence of any radiation (darkness current); $R_{экв}$ is the equivalent resistance of the photoconvertor; Δf is the bandwidth of the signal; k is the Boltzman constant ($k=1.38\times10^{-23}$ J/K); T is absolute temperature; N is the overhead noise coefficient related to the multiplication coefficient M.

According to the Stoletov law, I_c and F_ϕ photocurrents are

1

determined by the respective radiation intensities, F_c and F_Φ, arriving at the photoconvertor:

$$I_{c,\Phi} = \frac{\eta e}{h\nu} F_{c,\Phi},$$ (67)

where η is the quantum yield of the photoconvertor.

Solving simultaneously the equations (66) and (67), one can determine the intensity on the input of the reception system necessary for obtaining the required signal-to-noise ratio for the given frequency range:

$$F_e = k_1(n\Delta f) + k_1^2(n\Delta f)^2 + k_2(n\Delta f) + \frac{k_3 n\Delta f}{M^2 R_{\text{вх}}},$$ (68)

where

$$k_1 = \frac{2h\nu N}{m^2 \eta};$$
$$k_2 = \frac{4h^2\nu^2 N}{m^2\eta^2 e}\left(\frac{\eta e}{h\nu} F_\Phi + I_\tau\right);$$
$$k_3 = \frac{2kTh^2\nu^2}{m^2\eta^2 e^2}.$$

Here, k_1 characterizes the influence of the shot noise cuased by the signal, k_2 that of background radiation and darkness current, and k_3 that of thermal noise. When the product $n\Delta f$ increases, the largest influence will be that of the shot noise. In the limit,

$$n = \frac{m^2 \eta F_c}{4h\nu N\Delta f}.$$ (69)

The instantaneous value of the quantity n of a pulse system with direct amplification can be also determined by means of

2

(69), but in the place of m²/4 one has to put 1/2, and F_c represents the instantaneous value of the signal intensity.

The intensity of the background radiation being received by the photoconvertor is

$$F_\phi = S_{\text{обт}} \Omega \Delta\lambda B, \tag{70}$$

where $S_{\text{обт}}$ is the area of the objective; Ω is the viewing angle of the optical system of the receiving apparatus; $\Delta\lambda$ is the optical pass band of the filter, μm; B is the spectral density of the background radiation, $W/cm^2/\mu m/ster$.

The minimal permissible viewing angle is determined by the precision of the adjustment of the system in the direction of the source of radiation, and by the distortions of the wave front by atmospheric turbulencies.

Reception systems with direct amplification are distinguished by their simplicity, and they do not require that the radiation is coherent . The experimental studies showed [63] that the atmospheric effects do not have any practical influence on the operation of the system and their effect consists only in signal fluctuation.

Heterodyne Method

In this method two optical signals are directed onto the photoconvertor: (i) received signal carrying the information, and, (ii) local heterodyne signal. As the consequence of the difference in the frequencies of the two signals, a signal of difference frequency is generated on the output of the photoconvertor that contains the transmitted information.

3

Two identical lasers (one in the transmitter and one in the heterodyne) are used for the generation of the signals. At the same time, the frequency of the heterodyne is shifted in such a way that the total radiation energy arriving at the input is transformed into one side band, and the carrier frequency and the other side band are suppressed. In   practice, such a transformation of the input signal is realized only approximately and with a small coefficient of efficiency .

The heterodyne system for the frequency transformation is represented in Fig. 55 [63]. A larger portion of the radiative power is transformed into the side bands of the first order. The unwanted side bands and the carrier frequency are suppressed with a passive optimal filter. Phase modulation is realized by means of a rezonance modulator consisting of the KDR crystal with the transparent cover 4 and of the dielectric mirrors 2. As the optical filter 5, the role of which is to suppress the unwanted spectral components, one can use a Fabry-Perrault interferometer the pass band of which is identical with the working frequency range, or a birefringence filter.

Let e_c and e_r be the instantaneous value and the amplitude, respectively, of the electric field of the input light signal, and e_r and E_r be the respective quantities of the heterodyne signal, and ω_c and ω_r be the frequencies of these two signals. Then, if the front waves of these signals arriving on the sensitive surface of the photoconvertor are parallel and in phase, one can write

Fig. 55. Schematic drawing of the device for the transformation of the heterodyne frequency: 1- input heterodyne signal; 2- dielectric mirror; 3- teflon cylinder; 4- crystal; 5- optical filter; 6- output radiation

$$e_c = E_c \sin\omega_c t ;$$
$$e_r = E_r \sin\omega_r t ;$$
$$e = e_c + e_r = E_c \sin\omega_c t + E_r \sin\omega_r t .$$

Since the instantaneous intensity of the incident radiation $F(t)$ is directly proportional to e^2, we have

$$F(t) = \varkappa (E_c \sin \omega_c t + E_r \sin \omega_r t)^2 = \varkappa [E_c^2 + E_r^2 + E_c E_r \cos (\omega_r - \omega_c) t - E_c^2 \cos^2 \omega_c t - E_r^2 \cos^2 \omega_r t - E_c E_r \cos (\omega_r + \omega_c) t],$$

where $\varkappa$ is the proportionality coefficient.

The relation between the output photocurrent $I_{out}(t)$ and the intensity of the incident radiation has the form

$$I_{out} (t) = \frac{\eta e}{h\nu} F (t),$$

or

$$I_{out} (t) = \frac{\eta e \varkappa}{h\nu} [E_c^2 + E_r^2 + E_c E_r \cos (\omega_r - \omega_c) t - E_c^2 \cos^2 \omega_c t - E_r^2 \cos^2 \omega_r t - E_c E_r \cos (\omega_r + \omega_c) t].$$

5

The alternating component of the photocurrent of the
difference frequency $\omega_r - \omega_c$, is singled out by means of the
successive stages of the reception system,

$$I_{\text{вых}}(t) = \frac{\eta e n}{h\nu} E_c E_r \cos(\omega_r - \omega_c)t,$$

or

$$I_{\text{вых}}(t) = \frac{\eta e n}{h\nu} \sqrt{F_c F_r} \cos(\omega_r - \omega_c)t, \qquad (71)$$

where F_c and F_r are the intensities of the output signal and the
signal of the local heterodyne.

It follows from (71) that the larger the heterodyne power the
larger the output signal level. However, if there are frequency
side bands in the spectrum of the heterodyne radiation that lie
in the vicinity of the input signal frequency, and are within the
limits of the pass band of the successive electronic circuits,
the signal obtained as the result of the interaction of the
carrier signal with the signals of the side bands can surpass the
useful signal of the difference frequency F_p when the intensity
of the heterodyne signal is increased.

The main feature of the optical heterodyne reception consists
in the fact that the resulting signal of the difference frequency
can considerably exceed the level of internal noise. At the same
time, the shot noise caused by the heterodyne is larger than the
shot noise generated by the background radiation.

The signal-to-noise ratio for an ideal heterodyne reception
can be expressed as [63]

6

$$n = \frac{2I_r I_c M^2 R_{экв}}{2eI_r \Delta f/M^2 R_{экв}} = \frac{I_c}{e\Delta f} = \frac{I_c}{\frac{h\nu}{\eta}\Delta f}. \tag{72}$$

where I_c and I_r are the photocurrents caused by the output signal and heterodyne signal, respectively.

If the heterodyne reception system operates in the atmosphere, the parameters of the system get worse because of the the change of the spatial coherence of the radiation caused by the atmospheric turbulence. The operation of the system is also affected by the distortion of the wave front caused by the imperfection and aberration of the lenses, mirrors, modulators, and other optical elements. Nevertheless, the heterodyne method is distinguished by a high sensitivity and the possibility to solve the problem of the signal filtration by means of microwave, rather than optical elements.

The difficulties in the practical application of this method are the consequence of the rigorous requirements on the optical system of the reception apparatus resulting from the very small tolerated beam nonparallelism at the photoconvertor. Let us suppose that between the light beam of the input signal 1 and that of heterodyne 2 there is an angle γ (Fig. 56). Then

$$\sin \gamma = 1/d$$

where 1 is the difference in the paths of the beams, and d is the diameter of the input aperture of the optical system.
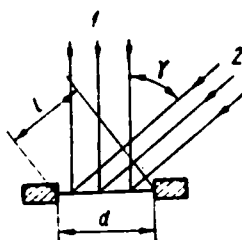
7

Fig. 56. The determination of the allowed angle between the beams of the incident and heterodyne radiations.

If the difference in the paths of the beams equals one half of the wavelength, their relative phase will equal 180°. This is the worse case when mixing the optical signals.

The tolerated degree of the nonparallelism of the two light beams incident on the sensitive surface of the receiver of the radiation energy can be expressed in the form

$$\sin \gamma \ll \lambda/(2d) \ .$$

Therefore, the angle γ should not exceed several angular seconds.

To achieve the precise angular coincidence of the input beam with the heterodyne beam, one can use a screen with the magnified image of the distribution of the fields of both beams in the distant region (Fig. 57). An effective mixing takes place if both beams overlap on the transparent mirror and on the screen. On the same screen one can also observe the influence of atmospheric effects on the spatial coherence of the received radiation.

A functional diagram of a broad-band receiving apparatus based on the heterodyne method is shown in Fig. 58. Here, F(t) represents the modulated optical radiation 1 containing the useful information. Modulation can be amplitude, phase, or

8

frequency. The module, the role of which is to generate the difference $\Delta\omega$ of the frequencies of the two lasers equal to the given intermediate frequency (UHF range), is connected with the heterodyne of the receiver, and not with the transmitter because the efficiency coefficient of this module is much less than one. To facilitate the operation of the module of the automatic frequency control, the tuning of the intermediate frequency $\Delta\omega$ is done at the input of the frequency-shift module.

Fig. 57. The mechanism for the angular adjusting of the input beam with the heterodyne beam: 1- incident radiation; 2- semi-transparent mirror (beam splitter); 3- screen; 4- diaphragm; 5- photoconvertor; 6- heterodyne and frequency transformer

Fig. 58. Functional scheme of a broad-band receiving apparatus: 1- modulated radiation from the transmitter; 2- semitransparent mirror; 3- photoconvertor; 4- AFC; 5- envelope-frequency detector; 6- output signal; 7- UHF generator of the intermediate frequency; 8- module of the heterodyne-frequency shift (transformation); 9- heterodyne

As the photoconvertor 3 one can use for a broad-band system either a photocell or a

photomultiplier with the running wave from the output of which the UHF signal is led off. The information-carrying signal is led off with the help of a diode with a small output capacitance.

The heterodyne principle can be used not only for the transformation of carrier frequency, but also for the transformation of the oscillations modulating the optical signal. The frequency of the modulating oscillations ω_m can be transformed into a new value $\omega_m \pm n\omega_r$ for which the usual photoconvertors intended for the range of small modulation frequencies can be used.
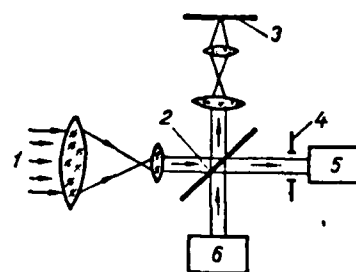
The requirements on the lasers for the optical heterodyne systems are much more rigorous than in the case of the reception systems with direct amplification. As the heterodyne of the pulse systems, one can use a low-power one-mode laser, and as the transmitter a high-power multi-mode laser with the phase synchronization, the radiation of which is equivalent to a pulse with one-frequency filling.

Because of the problems with the generation of the one-mode laser radiation of the transmitter and of the heterodyne, the possibilities of the heterodyne reception decrease considerably. However, if one succeeds with the creation of broad-band photoconvertors and other optical elements for the reception of CO_2 laser radiation ($\lambda = 10.6$ μm), efficient heterodyne systems for the infrared range could be built with their use.

10

Balance Method

In this reception method the input signal 1 (Fig. 59) and the signal from the supporting heterodyne ⁵ are led on the semi-transparent mirror 3, and then on the photoconvertors 2 and 4 [21,76].

Let us find the expression for the difference current at the output of the receivers assuming that the radiation refracted from, or transmitted through the mirror acquires an additional fixed phase shift of $\pm\phi$, and is attenuated m times. Let us introduce the following notation: - difference of phases of oscillations of the input signal and the of the heterodyne; e_1, e_2, F_1, and F_2 are the instantaneous values of the electric field and signal intensity at the input of the photoconvertor; i_1 and i_2 are the currents on the output of the receivers. Then

Fig. 59. Schematic diagram of the balance method of the reception of optical signal

$$e_c = E_c \sin \omega_c t; \quad e_r = E_r \sin (\omega_r t + \Phi);$$

$$e_1 = \frac{E_c}{m} \sin (\omega_c t + \varphi) +$$

$$+ \frac{E_r}{m} \sin (\omega_r t + \Phi - \varphi);$$

$$e_2 = \frac{E_c}{m} \sin (\omega_c t - \varphi) +$$

$$+ \frac{E_r}{m} \sin (\omega_r t + \Phi + \varphi);$$

$$F_1 = \varkappa e_1^2; \quad F_2 = \varkappa e_2^2; \quad i_1 = \frac{\eta e}{h\nu} F_1; \quad i_2 = \frac{\eta e}{h\nu} F_2;$$

$$i_1 - i_2 = \frac{\eta e \varkappa}{h\nu m^2} [E_c^2 \sin^2 (\omega_c t + \varphi) + E_r^2 \sin^2 (\omega_r t + \Phi - \varphi) +$$

$$+ 2E_c E_r \sin (\omega_c t + \varphi) \sin (\omega_r t + \Phi - \varphi) - E_c^2 \sin^2 (\omega_c t - \varphi) -$$

$$- E_r^2 \sin^2 (\omega_r t + \Phi + \varphi) - 2E_c E_r \sin (\omega_c t - \varphi) \sin (\omega_r t + \Phi + \varphi)].$$

1 1

Let us put $\phi = \pi/4$ and $m = \sqrt{2}$ to simplify the following mathematical considerations. Then

$$I_1 - I_2 = \frac{\eta e \varkappa}{2h\nu}\left\{E_c^2\left[\cos^2\left(\omega_c t - \frac{\pi}{4}\right) - \cos^2\left(\omega_c t + \frac{\pi}{4}\right)\right] + \right.$$
$$+ E_r^2\left[\cos^2\left(\omega_r t + \Phi - \frac{\pi}{4}\right) - \cos^2\left(\omega_r t + \Phi + \frac{\pi}{4}\right)\right] +$$
$$\left. + 2E_c E_r \cos\left[(\omega_r - \omega_c)t + \Phi\right]\right\}.$$

Neglecting the components of frequency larger than $\omega_r - \omega_c$, we obtain

$$i_{\text{mix}}(t) = \frac{\eta e \varkappa}{h\nu}E_c E_r \cos\left[(\omega_r - \omega_c)t + \Phi\right] =$$
$$= \frac{\eta e \varkappa}{h\nu}\sqrt{F_c F_r}\cos\left[(\omega_r - \omega_c)t + \Phi\right]. \qquad (73)$$

To realize this method of reception, one has to know the exact phase difference Φ. If the input-signal phase is constant, the average value of the phase can be measured in the course of a certain time interval. There are also arrangements [75] enabling to keep the difference Φ of the phases of the input signal and the signal of the supporting heterodyne equal to zero.

The Reception of the Frequency- and Phase-Modulated Oscillations

In all the cases of the reception of the frequency- and phase-modulated optical-range oscillations, the input signal is transformed into an amplitude-modulated signal that is subsequently detected by means of a photoconvertor. The schematic diagram of the reception system for the demodulation of the frequency-modulated signals is in Fig. 60 [28]. Its operation consists in the separation of a light beam into two parts of

12

equal intensity, the optical path of
each of them is modified. The beams
go through a semitransparent mirror
A. Each of the two beams go through
the air from the mirror A to the
mirror C. Then the signals are led to
photoconvertors.

Let L_A be the AFEDC path
traversed by the first part of the
splitted beam, and L_C is the ABC path
traversed by the second part of the splitted beam, and $\tau=(L_A-L_C)/(2c)$ is the time delay. Then the statistical characteristic
of the investigated frequency discriminator can be expressed by
the relation

Fig. 60. Schematic dia-
gram of the demodulation
of the frequency-modu-
lated signals

$$i_\Phi = k(E_m{}^2/2) \sin^2\Omega_0\tau , \qquad (74)$$

where i_Φ is the photocurrent from the photoconvertor; k is the
constant of proportionality between the photocurrent and the
radiation intensity; E_m is the amplitude of the field intensity
of the input signal; Ω_0 is the frequency of the carrier wave.

In this way, the output photocurrent of the investigated
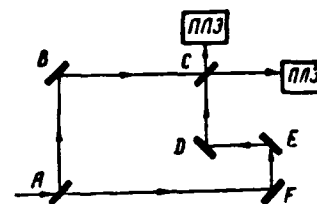discriminator changes when the frequency of the input signal is
changed.

(Original pages 132 & 133 missing here)

For $\lambda=0.7$ μm, $p_\text{w} = 2.8 \cdot 10^{-19}$ W/Hz, which is approximately 100 times more than in the case of the radio signals.

The main source of the quantum noise is the laser. Besides the noise generated by the fluctuations of the number of quanta of the induced radiation, an additional noise caused by the intermodal beats appears in the laser. This beat noise can be decreased by the use of one-mode lasers and by the increase of the quality of the optical resonator. However, as a matter of principle, the quantum noise of the generated signal cannot be eliminated completely, and it is the reason for the fluctuation of the number of electrons or of the photoconvertor's current. Therefore, the maximum sensitivity of the optical reception systems is determined by the optical noise and by the quantum efficiency of the photoconvertor.

At frequencies corresponding to the infrared range ($f=5\times10^{14}$ to 10^{12} Hz; $\lambda=0.6$ to 300 μm) one can transmit information in a very wide band. The largest values of the maximum information capacity that can be obtained in an idealized optical line for the information transmission in a 10^9 Hz wide band, amount to 10^{10} Hz for signals with the power of the order of 10^{-6} W [21].

These potential capabilities have been realized to some extent by means of the wideband photoconvertors with the internal amplification that gives pass bands several GHz wide. Such wideband systems can be used for the high-speed transmission of information with frequency or time compression of the channels.

19. PROPAGATION OF THE COHERENT OPTICAL RADIATION IN THE ATMOSPHERE

Among the main processes accompanying the propagation of the coherent optical radiation in the atmosphere, there belong the selective absorption and diffraction on the vapors of water, carbonic oxide, ozone, and methane, and on the tinest particles present in the atmosphere. In the range of heights up to 12 km, the radiation is absorbed mostly by the molecules of water vapor and carbonic oxide. The concentration of water vapor in the atmosphere depends on the geographic position, altitude, season of the year, and local meteorological conditions, and oscillates between 10^{-3} to 4 % (of volume). As the altitude increases, the content of water vapor contained in the atmosphere sharply decreases. The concentration of the carbonic oxide varies from 0.03 to 0.05 % of volume at the altitudes up to 20-25 km. At higher altitudes, the concentration is more uniform because of the vertical mixing of the atmosphere. Ozone concentration varies in a nonuniform way with the altitude. The main part of the atmospheric ozone is contained in the atmosphere layer at the altitude of 15-40 km, with the maximum concentration at about 30 km (more than 10^{-3} %). In the lower layers of the atmosphere, the ozone concentration amounts to 10^{-6}-10^{-5} %, and at the altitude of 65-70 km only traces of ozone are present.

Relatively intensive absorption lines correspond to the following intervals of the wavelength in μm:

for water vapor:

0.498-0.5114; 0.542-0.5478; 0.567-0.578; 0.586-0.606; 0.682-0.7304; 0.926-0.978; 1.095-1.165; 1.319-1.948; 1.762-1.977; 2.520-2.845; 4.24-4.4; 5.25-7.5;

for carbon oxide:

1.38-1.50; 1.52-1.67; 1.92-2.1; 2.64-2.87; 4.63-4.95; 5.05-5.35; 12.5-16.4;

for ozone:

0.6; 4.63-4.95; 8.3-10.6; 12.1-16.4.

Carbon oxide has an absorption line in the region of 47 μm; ozonous oxide has a very weak line at 4 μm and intensive absorption lines at 4.5 and 7.8 μm. Methane has two absorption lines in the interval of 3.1-3.5 μm and a narrow line at 7.7 μm.

The halfwidth of the radiation lines of the gas lasers is much smaller than the halfwidths of the absorption lines of atmospheric gases. That is why it is necessary to know with a high precision the position of the intensity and the form of the lines in the spectra of atmospheric gases to be able to estimate the absorption of the laser radiation in the atmosphere. The data on the absorption of optical radiation in atmospheric gases existing prior to the appearance of lasers have not been suitable enough for the estimate of the absorption of laser radiation in the atmosphere.

The attenuation of the radiation in the atmosphere is caused not only by its absorption, but also by its diffraction. The optical inhomogeneity of the atmosphere causes refraction, reflection, and scattering of the electromagnetic waves. If the dimensions of the particles floating in the atmosphere are small

16

with respect to the wavelength of the radiation, molecular scattering occurs. It is governed by the Rayleigh law according to which the intensity of scattering is inversely proportional to the fourth power of the wavelength. The molecular scattering is especially important in the visible and near infrared region of the spectrum. In the case of the particles the dimensions of which are comparable with the wavelength, one can observe diffractional scattering. If the dimensions of the particles are much larger than the wavelength, geometrical scattering takes place, which is mainly important in the infrared part of the spectrum.

There are particles of all sizes in the atmosphere, that is why all types of scattering take place. The largest scattering of the radiation occurs at small altitudes below 1000 m in urban areas where the atmosphere is heavily polluted with industrial smoke and soil dust. Besides absorption and scattering, also the bending of the light beams, random changes of the phase of the oscillations, fluctuations of the polarization of the radiation, etc., occur in the atmosphere. The refractive index of the medium varies because of small changes of the density of the air caused by small temperature gradients in the atmosphere; this results in the bending of light beams. This phenomenon has been known to astronomers for a long time. The dependence of the change of the refractive index on the change of temperature has the form [53]

$$\Delta n = - [(n-1)/T] \Delta T .$$
(78)

For n=1.0003 (refractive index of the air), T=300 °K, and $\Delta T = 1$ °K, one has $\Delta n \approx 10^{-6}$. The change of the refractive index Δn behaves as a random function of space variables and of time. The r.m.s value of the change of the refractive index as the function of height H can be described by an empirical formula

$$\overline{\Delta n^2} = 10^{-12} e^{-H/1600} , \qquad (79)$$

where H is in meters.

Experiments [53] showed that the maximum value of $\overline{\Delta n^2}$ occurs at the altitude of 300-400 m ($\sqrt{\overline{\Delta n^2}} \approx 10^{-6}$). At the distance D=30 km, such change of the refractive index causes an angular deviation, the r.m.s. value of which is $\sqrt{\Delta O^2} \approx 1$ μrad. The corresponding linear deviation is equal to 30 m. In the regions of the jumps of the refractive index, the size of which are large with respect to the beam cross-section, the phase front of the wave is distorted which results in the change of the direction of the beam. If the dimension of the region of the jump is much smaller than the beam cross-section, small segments of the wave front interact independently with the inhomogeneities, which leads to the appearance of dark and light spots in the plane of the objective of the receiving system. Because the atmosphere fluctuates continuously, the distribution of light and dark spots also changes continuously.

The described effects of the distortion of light beams can take place simultaneously, especially in the conditions of strong turbulence of lower layers of the atmosphere where the regions of

18

the inhomogeneity of the refractive index can change from a few millimeters to tens of meters. Therefore, the influence of the atmosphere on the propagation of visible radiation is a principal disadvantage of the optical system for the information transmission. Rain, fog, snow, and smoke increase the absorption of the radiative flow and decrease maximum range of communication lines.

At present, there are no analytical methods for the calculation of absorption of coherent radiation in the atmosphere; that is why one uses the results of experimental investigations. Thanks to the sufficiently large quantity of data available on the propagation of coherent radiation in the atmosphere, the transmission of radiation can be estimated with a very high precision. According to the data of [8], the coefficient of the absorption of radiation of the wavelength of 1.15 μm, measured in a flask and in natural conditions, equals 0.3 per 1 mm of the precipitated water. For laser radiation of the wavelength of 3.93 μm, the absorption coefficient in the layer adjacent to the ground equals 6 dB/km. In this case, the influence of methane plays a considerable role, which is usually not taken into account when the absorption of the radiation of nonmonochromatic sources is calculated. The centers of methane absorption lines are identical with the wavelength of 3.93 μm.

According to the data of [76], absorption coefficient of the helium-neon laser with the wavelength of 1.152 μm changes approximately in a linear way from 3 to 10 dB/km when the relative humidity of the air changes from 10 to 40 % (at   sea

19

λ=3,5мм
λ=0,63мм
Уровень шумов (3,5мм) — 2
Уровень шумов (0,63мм) — 3
Время — 4
а

λ=3,5мм
λ=0,63мм — 1
Время — 4
б — b

λ=0,63мм
λ=3,5мм — 1
Время — 4
в — c

Fig. 61. Attenuation of the coherent radiation in the atmosphere.

1- μm; 2- Noise level (3.5 μm); 3- Noise level (0.63 μm); 4- Time
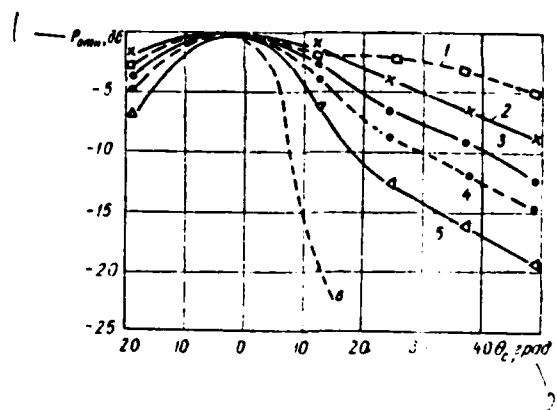

Fig. 62. Graph of the change of the angle of divergence of the beam during snowfall (λ=0.6328 μm, distance of 2.6 km).

1-   dB; 2- Θ_c, degree

level). There, one can find the graph of the dependence of the absorption coefficient σ for the radiation with the wavelength of

20

Table 18. Attenuation of the coherent radiation of wavelength of 0.6328 μm under various meteorological conditions

2- Осадки	3- Скорость ветра, м/сек	4- Дальность видимости, км	5- Относительная влажность, %	6- Температура, °C	7- Ослабление сигнала, дб
8- Дальность 900 м					
9- Ясно	2	2	68	7,5	16,6
»	2	3	62	11,5	17,7
»	2	—	41	10	17
»	—	>8	43	12,5	18
»	3,5	>10	34	10	13
10- Сильный дождь	—	2	74	7	20,7
11- Слабый дождь, небольшой туман	—	1	85	6	50,7
12- Туман	—	1	75	8	33
»	—	0,5	75	2,5	52,8
»	—	0,3	73	3,5	95
»	—	0,05	67	7	116,2
14- Дальность 5600 м					
9- Ясно	2	8	35	23	45,2
»	2	5	72	11	63,5
»	2	3	62	19	58,5
13- Пасмурно	—	2,5	78	18	73,2
»	—	2	68	22	81,4

1- Meteorological conditions; 2- Precipitation, 3- Wind velocity, m/s; 4- Visibility range, km; 5- Relative humidity, %; 6- Temperature, °C; 7- Signal attenuation, dB; 8- Distance 900 m; 9- Clear sky; 10- Heavy rain; 11- Light rain, light fog; 12- Fog; 13- Cloudy; 14- Distance 5600 m

0.6943 μm on the meteorological visibility range d. Namely, at d = 1, 10, and 50 km, the value of σ is 20, 2, and 0.3 dB/km.

The influence of mild rain on the transmission of radiation with the wavelengths of 0.63 and 3.5 μm over the distance of 2.6 km is visible from Fig. 61a. Heavy rain causes even larger attenuation. Figs. 61b,c show the influence of fog. Fig. 61b corresponds to fog consisting of small droplets of diameter of 1 μm and less. This can explain the much larger

21

attenuation of the wavelength of 0.63 μm as compared with 3.5 μm wavelength. The signal level under good meteorological conditions is assumed to be 0 dB in all three cases [69]. The influence of snowfall is illustrated in Fig. 62. During the snowfall, the light beam diverges and the energy of coherent radiation decreases. Curve 5 of Fig. 62 corresponds to a light snowfall, and does not differ much from the curve corresponding to a clear sky. Curves 1-4 correspond to the increasing intensity of the snowfall and show that a snowstorm spreads the light beam and attenuates the radiation. The signal attenuation at the maximum of curves 1 to 5 amounts to 17.9, 15.6, 13.6, 5.0, and 3.5 dB/km. Curve 6 does not taken into account the influence of the atmosphere at all.

Of some interest is also data presented in [81] on the attenuation of the coherent radiation at the wavelength of 0.6328 μm under various meteorological conditions (Table 18).

20. THE SELECTION OF THE MAIN ELEMENTS OF OPTICAL LINES AND OF THE SYSTEMS FOR INFORMATION TRANSMISSION

A generalized scheme of operation of an optical system for information transmission is given in Fig. 63. Laser 3 together with the pumping system 2 and power supply block 1 has the role of the source

(Original pages 140-143) missing here)

22

21. THE PURPOSE AND THE CLASSIFICATION OF THE DEVICES TO CONTROL THE ORIENTATION OF LASER BEAMS

The work on diverse information systems using lasers resulted in the development of the methods and means of the control of the orientation of the laser beam that are characterized by a high speed of deflection with high resolution. Among the potential areas of application of these methods and means there belong:

1. scanning in the optical lines of information transmission, in the systems for target detection and optical localization;

2. raster scanning of the laser beam in the systems for the generation of videosignals;

3. line scanning in the systems of projectional television;

4. line scanning in the systems of videorecorders for television or radar;

5. scanning of a laser beam during writing, reading, or erasing in the systems for the processing of optical information, and in the optical calculating machines.

Basic requirements on the devices controlling the deflection of a laser beam are: high speed and high precision of the beam deflection, small loss of the beam energy, small phase distortions of the front of the optical wave, acceptable magnitude of the control voltage, and linearity of the deflection.

The devices for the laser beam deflection can be divided into two groups: (i) external with respect to the source of the radiation, and (ii) internal, integrated with the source of the laser radiation. The external devices use controlled reflectors,

23

controlled refractive systems, and refractive elements based on interference or polarization. The principle of the operation of internal devices is based on the selection of suitable types of oscillations in the optical resonator of the laser.

Depending on the character of the deflection of the beam, one distinguishes devices for continuous deflection according to the predetermined program, and devices for discrete deflection. In this chapter only the devices belonging to the first group are investigated.

The problems of the control of the laser beam orientation are relatively new and are attracting ever increasing interest. That is why the methods and means of the deflection of the beam are being continuously perfected and their present development is far from being finished.

22. CONTROL OF THE LASER-BEAM ORIENTATION BY MEANS OF REFLECTORS

One of the first methods to control the orientation of the light beam was a mechanical or electromechanical scanning based on the reflection of light from a rotating mirror. This method is used, e.g., in loop-type oscillographs and photoregistrators with a rotating mirror.

A loop-type oscillograph contains a mirror mounted on a conductive filament suspended in constant magnetic fields. When a current flows through the filament, the mirror deviates, and the light beam reflected from the mirror deflects. Devices of this type
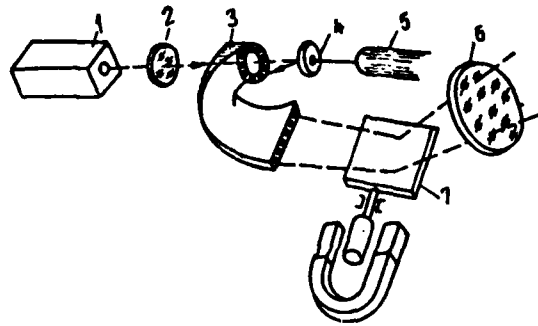
Fig. 65. Schematic drawing of a deflection device with the piezoelectric vibrator:

1- laser; 2- collimator; 3- fiber optics; 4- vibrating mirror; 5- piezoelectric material; 6- lens; 7- vertical-scanning block

are used in the frequency range of 0-13 kHz. Maximum frequency is determined by the momentum of inertia of the filament-mirror system.

Utilizing the mechanical resonance of the system supporting the mirror, one can achieve large angular beam deflections at very low power of the controlling signal. This principle is realised in a scanning device consisting of a mirror fixed to one of the ends of a torsional tuning fork. This device enables the scanning of a beam within the range of a 5° angle with a frequency of 1600 Hz at mirror dimensions of 5x5 mm.

Instead of the torsional tuning fork, one can use piezoelectric material, which alternately enlarges and shrinks under the influence of electrical field. Applying suitably varying electrical fields, the mirror attached to the piezoelectric material will perform circular scanning of the laser beam. In one of the experimental samples, the resonance frequency was 15.75 kHz. The circularly scanned beam is aimed at a circular end of fiber optics 3 (Fig. 65), the other end of which is elongated. In this
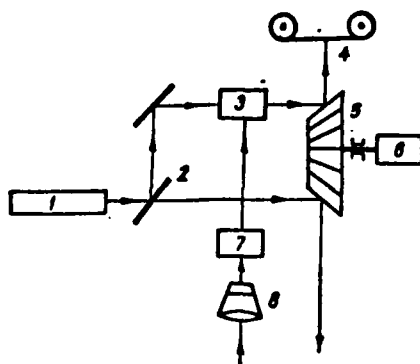
Fig. 66. Schematic drawing of the principle of the device for the night airborne reconnaissance

way, the circular scanning is transformed into a linear one, in the particular case, into a horizontal one. In such a case the conversion excludes the time of reverse movement of the beam.

Vertical scanning can be achieved by means of a mirror connected to a galvanometer. Under the influence of the magnetic field, the mirror moves up and down with the frequency of 60 Hz. In this case, the frequency of the vertical scanning equals 30 pictures/s for 525-line scanning [50].

Let us investigate the possibilities of the use of rotating mirrors. Using them, one can achieve very large speeds of scanning; however, it is impossible to change these speeds rapidly. Because the mirror rotates in one direction, scanning is governed by a sawtooth law in such way that each plane of the mirror corresponds to one scanning line. Maximum scanning speed is limited by the strength of the mirror drum. Moreover, at high speeds, the mirror planes undergo distortions, so that optical correction must be made.

Maximum speed of a mirror made of beryllium is believed to be 500 m/s; at this speed the six-face rotating mirror ensures the frequency of 31 kHz assuming that the reverse motion of the beam

lasts 10 % of the full scanning period.

An example of the use of rotating mirrors is the device for night airborne reconnaissance as depicted in Fig. 66 [31].

Continuous-wave radiation of laser 1 is divided with the help of semitransparent mirror 2 into two beams that are aimed at the rotating mirror while one beam has to go through electrooptical modulator 3. Mirror 5 driven by motor 6 has the form of a six-face cut pyramid. It serves for the scanning of the laser beam in the range of 30-40° in the plane perpendicular to the direction of the airplane flight. The radiation reflected from the Earth surface is received by optical system 8 and led to photomultiplier 7. Detected signals, the amplitude of which depends on the reflective properties of the scanned territory, modulate the initial laser radiation. Optical signals are then led from the output of the modulator on photoregistering device 4.

The system has the following parameters: Maximum flight speed of 1100 km/h; ratio of the speed to the flight altitude of 0.05-2 rad/s; angular resolution of 0.3-0.5 μrad; optical-system focal length of 57 mm; weight of 70 kg; power consumption of 1 kW; and the length of photographic film of 30 m.

Another device with mechanical scanning (Fig. 67) contains two three-face mirrors 2 attached to a common axis driven by the motor 1. The mirrors are mutually rotated by 60°. The radiation of laser 8 is collimated with lens 7, and aimed at the rotated mirrors with the help of auxilliary mirrors 4 and 6, and lens 3. The beams
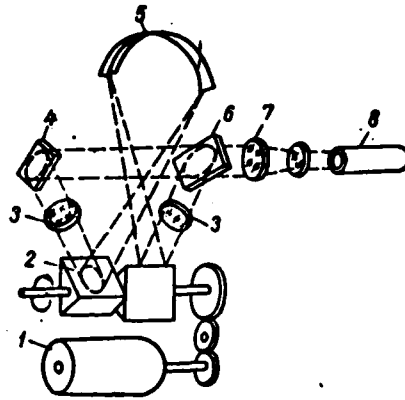
27

Fig. 67. Schematic drawing of the deflection device with mechanical scanning

reflected alternately from each face of the mirrors cover the scanning in a sector of 120°. The path of the beam scanning is denoted by cipher 5. Diameter of the spot equals 5 μm. Scanning speed can reach 360 diameters of the spot per 1 second [50].

23. CONTROL OF THE LASER BEAM ORIENTATION BY MEANS OF THE REFRACTIVE DEVICES

The principle of the operation of the controlled refractive devices for the change of the orientation of the laser beam is based on the control of the refraction of radiation in an inhomogeneous medium.

If there is a gradient of the refractive index in the direction perpendicular to the direction of radiation, a normally incident beam deviates from its original position in the direction of the increase of refractive index. Let us assume that the beams entering the refractive medium at the points A_1 and A_2 (Fig. 68) are in phase. Under small changes of the refractive index

(Original pages 148-159 missing here)

Chapter 5

SYSTEMS FOR MEASURING THE PARAMETERS OF MOVING OBJECTS

24. PRINCIPLES OF THE RANGE FINDERS AND THE RESPECTIVE FORMULAS

The development of lasers capable of generation of light
pulses of very high power and of short duration enabled to build
precision optical range finders based on the principle of the
radio range finders, but differing from them by high
directionality and high precision of operation. Small angular
divergence of laser beams used in optical distance finders makes
it more difficult to locate the target. In spite of this, such
range finders are used together with radio range finders because
they have several principal advantages. One of them is a large
stability to disturbances, which is a consequence of the high
directionality and monochromaticity of the radiation. To create
efficient disturbances, it would be necessary to generate a
perturbing signal of frequency identical to that of the laser
signal and oriented in the same direction. A laser range finding
device can operate at a much smaller power than a radio range
finder, and, at the same time, determine the distance and the
angular dimensions of the object with a higher precision. It is
assumed that with the help of an optical range finder one can
obtain a more detailed image of the object, even the trace of its
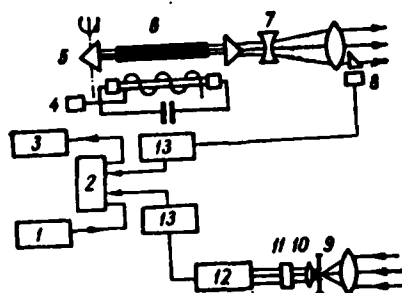contour.

Fig. 74. Schematic diagram of the optical range finder with a laser: 1- generator of time marking pulses; 2- strobo-scopic mechanism; 3- pulse counter; 4- trigger of the pumping lamp; 5- rotating prism; 6- laser crystal (active substance); 7- collimating optical system; 8- photodiode; 9- diaphragm; 10- lens; 11- filter; 12- photomultiplier; 13- amplifier.

Lasers operating both in the pulse and continuous regimes can be used in optical range finders; this will determine the construction of the device.

Schematic diagram of a laser range finder is shown in Fig. 74. Laser 6 together with collimator 7 direct powerful pulses of short duration to the object the distance of which is to be measured. Time origin for the distance measurement is set by triggering the counter of time marking pulses 3 generated by generator 1. This is ensured by photodiode 8 to which a small part of the sonding laser signal is led. After the amplification, the current from the photodiode is brought to stroboscopic mechanism 2 which switches on the pulse counter.

The light pulse reflected by the object is received by the receiving set consisting of the optical system, filter 11, photomultiplier 12, and amplifier 13. The current pulse from the output of the amplifier proceeds to the stroboscopic mechanism that locks the pulse

counter. The number of time marking pulses arriving at the counter from the moment of sending the laser pulse to the moment of receiving the reflected pulse is proportional to the measured distance. The peculiarity of this device consists in the fact that the result of the distance measurement is available immediately after each measurement.

Laser range finders using continuous-wave radiation are based on a different scheme. To measure the distance, the laser radiation of the carrier frequency is amplitude modulated with a sinusoidal signal and directed to the object. The reflected radiation is received by an optical system and a photomultiplier. The distance is determined by the phase shift of the transmitted and received signals (at the frequency of the modulating signal).

Let us investigate the equations determining the maximum range of operation of an optical laser range finder working in the pulse regime. Let us assume that the whole radiative flow irradiated by the laser reaches the object (this assumption is justified because the angular divergence of the beam is small and the measured distance relatively small). If the dimensions of the object are small with respect to the distance between the object and the range finder, one can also assume that the object reradiates the received energy in a similar way as a point source; and the scattering from the surface of the object is governed by the Lambert law. Under such assumptions, the energy of the received signal is

$$E_{np} = P_{np} t_{\text{в}} = \frac{P_{\text{и}} \rho t_{\text{и}} \cos \alpha \tau_{\text{в}}^{!} S_{\text{опт}} \tau_{\text{опт}}}{\pi D^{\text{в}}},$$

(106)

31

where P_{np} is the power of the received signal; P_s is the peak power of the radiation; t_u is the duration of the pulse; ρ is the coefficient of the diffuse reflection from the object; a is the angle between the direction to the object and its surface normal; τ_a is the transmission coefficient of the atmosphere for the unilateral propagation of the laser radiation; D is the distance of the object; S_{onr} is the area of the objective of the optical system; and τ_{onr} is the transmission coefficient of the optical system.

Let us assume that the received signal reaches the receiving set realized by a photomultiplier. Then the mean number of the photoelectrons released from the cathode of the photomultiplier is

$$\overline{m}_t = \frac{\eta E_{np}}{h\nu}, \tag{107}$$

where η is the quantum yield and ν is the mean working frequency.

The required number of photoelectrons is determined by the inequality

$$(\overline{m_t})_{min} \geq n \geq 1 ,$$

where n is an integer selected on the basis of the following considerations. The number of electrons m actually arriving at the anode in any of the measuring intervals fluctuates around the quantity $\overline{m_t}$, while the probability P of finding the value m is given by Poisson distribution:

$$P(m;\overline{m}_t) = (\overline{m_t})^m/m! \ exp(-\overline{m_t}) .$$

32

Therefore, the signal on the output of the photomultiplier will fluctuate because it is proportinal to the number of electrons arriving at the anode in the preceding time interval. Besides this the output signal equals zero unless the number of electrons in the photomultiplier exceeds the value n . The probability that the circuit will work at the end of any interval $t_н$ is

$$P(m > n; \ \overline{m}_t) = \sum_{m=n}^{\infty} \frac{(\overline{m}_t)^m}{m!} e^{-\overline{m}_t}. \tag{108}$$

From eq. (108), one can obtain quantity $(m_t)_{min}$ corresponding to the given a priori probability $P_з$. Substituting the value $(m_t)_{min}$ into eq. (107), we will obtain

$$(\overline{m}_t)_{min} = \frac{\eta \lambda P_н \rho l_н \cos a \tau_a^2 S_{опт} \tau_{опт}}{\pi D_{max}^2 ch},$$

which results in

$$D_{max} = \tau_a \sqrt{\frac{P_н \rho \gamma l_н \cos a S_{опт} \tau_{опт} \gamma}{\pi (\overline{m}_t)_{min} h\nu}}. \tag{109}$$

As the input data for the calculation, one can use:

$E = P_н l_н = 50 \cdot 10^{-3} \ \ J \ \rho = 0,1 \div 0,2; \ S_{опт} = (0,75 + 1) \cdot 10^{-3} \ м^2;$
$\eta = 0,03$ (at $\lambda = 0,69 \, \mu m$); $\tau_{опт} = 0,4 \div 0,5;$
$\frac{hc}{\lambda} = 2,8 \cdot 10^{-19} \ J$ (for $\lambda = 0,69$ microns)

The distance formula (109) can be used provided that the influence of the background radiation and the darkness current is negligible. However, in   practice, a certain number of photoelectrons are always created by the darkness current and by the radiation of external sources (Sun, Moon, stars,

33

clouds, warmed objects) arriving in the viewing field of the optical system of the receiving set that is called background radiation.

The background radiation is incoherent and of broadband character, occupying the visible and the infrared regions of the electromagnetic spectrum. The main source of the background radiation during the day is the radiation of the Sun reflected by the object, the distance of which is being measured and its vicinity. The energy $E_{np.\phi}$ received by the receiving part of an optical range finder depends on its viewing field, on the characteristics of the medium in the vicinity of the object, and on the meteorological conditions.

Let us assume that the viewing field of the receiver contains a part of the elongated background with the diffusion function $F(\phi,\psi)$, where ψ is the angle between the direction of the incident radiation and the normal to the scattering surface, and ϕ is the angle between the axis of the viewing field and the same normal. To simplify the calculations, function $F(\phi,\psi)$ is often put equal to one.

The energy of the received background radiation can be determined by means of the formula

$$E_{np.\,\phi} = \frac{B_{\lambda\Phi}\Delta\lambda_{\,b\ell_{H^2}\phi}S_{onT}\tau_{oH}\tau_{\bullet}{}^{\mu}F\,(\mp\;\psi)}{\pi}\,,$$

$$(110)$$

where $B_{\lambda\Phi}$ is the spectral illuminance of the background surface in the target region, $\frac{w/m^2}{\Lambda\cdot\AA}$; $\Delta\lambda_{\Phi}$ is the width of the pass band of the optical filter, $\AA$; ρ_{Φ} is the reflection coefficient of

34

the target surface; Ω is the solid angle of the viewing field of the optical system of the receiver, ster; and $t_{\text{и}}$ is the interval of observation equal to the duration of the pulse, s. Transmission coefficients of the atmosphere, τ_a, and of the optical system, $\tau_{\text{опт}}$, are assumed to be the same for the working signal and for the background radiation.

The mean number of the photoelectrons generated by the background radiation and registered during the interval $t_{\text{и}}$, is given by the formula:

$$\overline{m}_\phi = \frac{E_{\text{пр. }\phi}\eta}{h\nu} = \frac{t_{\text{и}}B_{\lambda\phi}\rho_\phi\Delta\lambda_\phi S_{\text{опт}}\Omega\tau_a\tau_{\text{опт}}\eta F(\varphi, \psi)}{\pi h\nu}. \tag{111}$$

The dc component of the cathode current of the photo-multiplier generated by the background radiation is

$$I_\phi = \frac{B_{\lambda\phi}\rho_\phi\Delta\lambda_\phi S_{\text{опт}}\Omega\tau_a\tau_{\text{опт}}\eta F(\varphi, \psi)\,e}{\pi h\nu}. \tag{112}$$

To determine the maximum range of operation of a range finder while taking into account the effect of the background radiation, let us find the r.m.s value of the shot-noise current $I_{\text{др}}$ at the cathode. In the case of large amplification coefficient of the photomultiplicator, the shot noise is much larger than the thermal noise that can, therefore, be neglected. Then

$$I_{\text{др}} = \sqrt{2eI\,\Delta f},$$

where Δf is the pass band of the circuits hooked up to the

35

photomultiplier for the given pulse duration; I is the current flowing through the photomultiplier,

$$I = I_{np} + I_\phi + I_\tau;$$

I_{np}— is the current of the working signal; I_ϕ is the current caused by the background radiation; and I_τ is the darkness current.

The signal-to-noise ratio in the cathode circuit is given by the expression:

$$n = I_{pr}/I_{dr} = I_{pr}/\sqrt{[2e(I_{pr}+I_\phi+I_\tau)\Delta f]} \ . \qquad (113)$$

The same relation will hold in the anode circuit because signal and noise are amplified in the same way.

If the background radiation predominates, $I_\phi \gg I_{np} + I_\tau$ which results in

$$n = \frac{I_{np}}{\sqrt{2eI_\phi \Delta f}}. \qquad (114)$$

Substituting into (114) for I_ϕ from formula (112), and for I_{np} the quantity

$$I_{np} = \frac{E_{np}\tau_\ell}{h\nu l_{\mu}} = \frac{\eta P_{\mu}\rho \cos \alpha \tau_a^2 S_{on\tau}\tau_{on}\ell}{h\nu \pi D^2} \ , \qquad (115)$$

results in

36

$$n = \frac{\tau_i P_{\text{и}} \rho \cos a \tau_a^2 S_{\text{опт}} \tau_{\text{опт}}}{h \nu \pi D^2 \sqrt{2\Delta f \dfrac{B_{\lambda \Phi} \rho_\Phi \Delta \lambda_\Phi S_{\text{опт}} \Omega F(\varphi, \psi) \tau_a \tau_{\text{опт}} \eta}{\pi h \nu}}},$$

which leads to

$$D = \left(\frac{P_{\text{и}} \rho \cos a}{n}\right)^{\frac{1}{2}} \left(\frac{\tau_a^3 \tau_i S_{\text{опт}} \tau_{\text{опт}}}{2\pi \rho_\Phi h \nu B_{\lambda \Phi} \Delta \lambda_\Phi \Omega F(\varphi, \psi) \Delta f}\right)^{\frac{1}{4}}.$$

(116)

To find the distance by means of formula (116), it is necessary to know the quantity $B_{\lambda \Phi}$, which is being determined experimentally. In the vicinity of the earth surface, $B_{\lambda \Phi}$ is of the order of $0.1 \, \frac{\omega/m^2}{Å}$ in the wavelength range of 0.840-0.900 μm [51].

When aiming directly at the source of radiation, formula (110) changes to

$$E_{\text{пр}. \Phi} = \frac{B_{\lambda \Phi}^* \Delta \lambda_\Phi l_{\text{и}} S_{\text{опт}} \tau_{\text{опт}} \tau_a \Omega}{\pi},$$

(117)

where $B_{\lambda \Phi}^*$ is the illuminance of the receiving lens of the objective caused by the source of radiation.

The values of the illuminance caused by the sources of background radiation in the spectrum range $\Delta \lambda_\Phi = 10 \, Å$ in wavelength range of ruby and helium-neon lasers are given in Table 20 [74].

At night, the main sources of the background radiation are warmed objects. The density of the radiative energy flow irradiated in the spectral range $\Delta \lambda$ by warmed objects that can be considered to be black bodies is given by the formula

37

Table 20. Illuminance caused by the sources of background radiation

— Источник излучения	2- Облученность (вт/см²) в полосе 10 Å при длине волны λ, мк	
	0,6943	1.150
3 - Солнце	$1{,}3 \cdot 10^{-4}$	$5{,}2 \cdot 10^{-6}$
4 - Луна	$1{,}3 \cdot 10^{-10}$	$5{,}2 \cdot 10^{-11}$
5 - Ночное небо (звезды)	10^{-12}	$4{,}2 \cdot 10^{-14}$
6 - Яркая звезда (Сириус)	$1{,}2 \cdot 10^{-13}$	$2{,}8 \cdot 10^{-16}$

1- Source of radiation; 2- Illuminance (W/cm²) in the 10 Å range for wavelength λ, μm; 3- Sun; 4- Moon; 5- Night sky (stars); 6- Bright star (Sirius)

$$R = \frac{C_1 \epsilon \, \Delta\lambda}{\lambda_0 \left(e^{\frac{C_2}{\lambda_0 T}} - 1\right)} \frac{W}{cm^2},$$

(118)

where C_1 and C_2 are constant coeficients ($C_1 = 3.74 \times 10^{-12}$ Wcm²; $C_2 = 1.439$ cm deg); λ_0 is is the wavelength of the received laser radiation, μm; ϵ is the coefficient of irradiation of the surface of warmed body, which can be considered in the first approximation independent of the body temperature, direction of radiation, and wavelength.

Formula (110) has in the investigated case the form

$$E_{np.\phi} = \frac{C_1 \epsilon \, \Delta\lambda_\phi \, l_u S_{ont} \tau_{unt} \tau_a S}{\lambda_0 \left(e^{\frac{C_2}{\lambda_0 T}} - 1\right) \pi D^2},$$

(119)

where S is the surface of the warmed object perpendicular to the optical axis of the receiving set and being in its viewing field, cm².

Using expression (116), one can estimate the influence of various factors on the maximum operating range of an optical range finder. The distance is proportional to the quantity $P_\text{м}^{1/2}/\Delta f^{1/4}$. In the pass band of an optical filter, $\Delta f = \frac{1}{t_\text{м}}$, therefore, it is expedient to irradiate the energy in the pulses of large amplitude and short duration. Contrary to the photon limitation, when the distance is proportional to the quantity $S_\text{опт}^{1/2}$, in the case of background limitation the distance depends on $S_\text{опт}^{1/4}$.

Let us investigate the case when the operation range is limited by the backward scattering of the radiative flow in the direction of the receiver. The backward scattering has special value for the propagation of the radiation in the fog, when part of the radiation passes through a layer of the atmosphere while the other part is reflected as a consequence of the scattering by fog particles.

Fig. 75a represents the light beam irradiated by the transmitter, and the viewing field of the optical system of the receiver. They do not overlap in the vicinity of the range finder, but at a certain distance D_0 from it, radiative flow refracted by a part of the atmosphere (shaded area of the Figure) falls into the viewing field of the receiver. In the case of fog of uniform density, the signal caused by the scattering of the atmosphere changes according to the ratio D/D_0 in the manner illustrated in Fig. 75b [39].

The signal generated by the atmospheric scattering in the direction of the receiver has a considerable influence on the
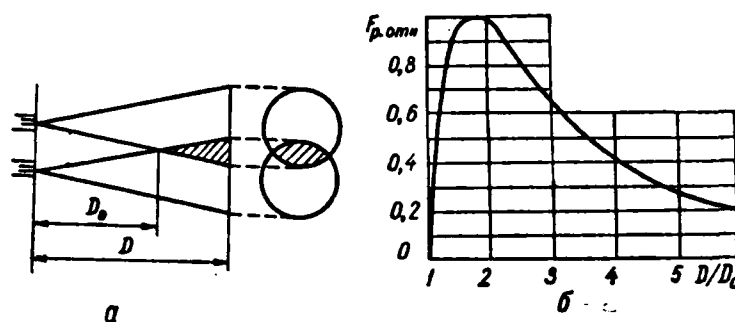
Fig. 75. Light beam irradiated by the transmitter, viewing field of the optical system of the receiver, and the magnitude of the signal caused by the backward scattering in the atmosphere.

threshold level of the receiver, and, therefore, on the maximum operating distance of the optical range finder. Let us, therefore, investigate the dependence of this signal on the distance and the parameters characterizing the fog density. It is possible to assume that the backward scattering, i.e. the scattering towards the source of radiation is isotropic, and that the light beam irradiated by the laser, and the beam back-scattered towards the receiver do not overlap at long distances. Under these conditions the radiative flow at the distance D from the laser irradiating the flow $P_{\text{и}}$ is determined by the formula

$$P_D = P_{\text{и}} e^{-kD} = P_{\text{и}} \cdot 10^{-\frac{\sigma D}{10}}, \tag{120}$$

where k is a constant characterizing the nature of the fog; σ is

40

the attenuation of the radiative flow in dB per unit length related to the coefficient k by means of the relation $k = 0.043\sigma$.
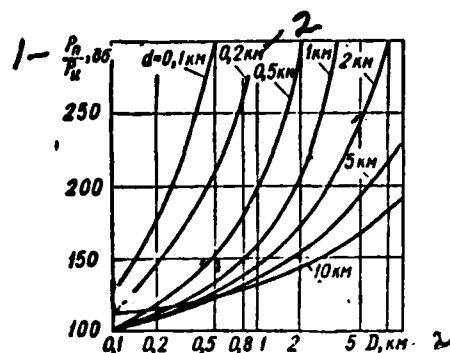

Fig. 76. The dependence of the relation $\frac{P_\text{п}}{P_\text{и}}$ on the distance D for various values of the visibility range.

1- $\frac{P_\text{п}}{P_\text{и}}$ dB; 2- km

Towards the receiver, the radiative flow created as a result of the reflection from a layer of the atmosphere $ct_\text{и}$ thick is scattered. The magnitude of the radiative flow refracted by such a layer at the distance D towards the receiver and falling on the optical system with the input mirror area $S_\text{опт}$ is determined by the expression

$$P_\text{p} = \frac{kP_D ct_\text{и} S_\text{опт}}{4\pi D^2} = \frac{kct_\text{и} S_\text{опт}}{4\pi D^2} P_\text{и} \cdot 10^{-\frac{\sigma D}{10}}. \qquad (121)$$

Before reaching the receiver, the radiative flow refracted by the atmosphere is attenuated because the reflected radiation goes through a layer of fog of the thickness D. That is why the radiative flow,

$$P_\text{p} = P_\text{и} \frac{0{,}043\sigma ct_\text{и} S_\text{опт}}{4\pi D^2} \cdot 10^{-\frac{2\sigma D}{10}}. \qquad (122)$$

41

falls on the input of the receiver.

The following approximate dependence on the optical visibility range can be used for σ:

$$\sigma \approx 20/d \ .$$

That is why we finally obtain

$$P_n = P_{\text{и}} \frac{0{,}86 c t_{\text{и}} S_{\text{опт}}}{4\pi} \cdot \frac{1}{dD^2} \cdot 10^{-\frac{4D}{d}} \tag{123}$$

The first factor in the expression (123) represents properties of the range finder while the second factor is a function of the distance.

The curves in Fig. 76 represent the dependence of $\frac{P_n}{P_{\text{и}}}$ on the distance for two different values of the visibility range. The parameters of the range finding system are: $S_{\text{опт}} = 50 \ cm^2$; $t_{\text{и}} = 10^{-8}$ s.

The signal generated by the atmospheric scattering determines the current of the photoconvertor:

$$I_{\text{a}} = \frac{\eta e P_n}{h\nu} \ .$$

The effective value of the noise current generated by the atmospheric scattering is determined by the formula

$$I_{\text{ш}} = \sqrt{\frac{2 e I_n}{t_{\text{и}}}} = \sqrt{\frac{2 e^2 P_n \eta}{h\nu t_{\text{и}}}} \ . \tag{124}$$

Substituting into this formula the expression (123) for $P_{\text{ш}}$ one obtains

$$I_{\text{эф}} = \frac{1}{2D} \cdot 10^{-\frac{2D}{d}} \sqrt{P_{\text{и}} \frac{2e^2 \eta}{h\nu} \cdot \frac{0,86 c S_{\text{опт}}}{\pi d}}.$$ (125)

On the other hand, the photocurrent generated by the useful signal can be expressed as

$$I_{\text{c}} = P_{\text{и}} \frac{\rho S_{\text{опт}} \gamma e \cos \alpha}{4 \pi h \nu D^2} \cdot 10^{-\frac{4D}{J}}$$ (126)

when taking into account the adsorption caused by atmospheric scattering ($\tau_{\text{опт}}$ and $\cos\alpha$ were assumed to be equal to one).
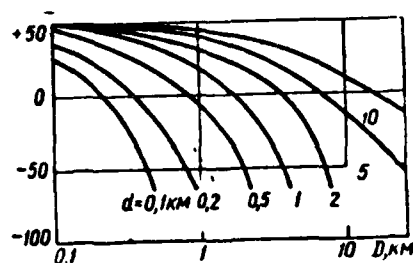

Fig. 77. Dependence of the relation $\frac{I_{\text{c}}}{I_{\text{эф}}}$ on the distance D for various values of the visibility range.

The relation of the photocurrent generated by the useful signal to the effective value of the photocurrent generated by the atmospheric scattering.

$$\frac{I_{\text{c}}}{I_{\text{эф}}} = \rho \sqrt{\frac{P_{\text{и}} S_{\text{опт}} \gamma d}{21,6 h \nu c} \cdot \frac{10^{-\frac{2D}{d}}}{D}}.$$ (127)

It is necessary to note that the duration of the pulse, $t_{\text{и}}$ does not affect the obtained formula. This can be explained by

the fact that is was assumed to be equal to the time resolution of the receiver.

Fig. 77 shows the graphs of the dependence of the ratio $\frac{I_c}{I_{\omega}}$ on the distance D for various values of the visibility range d for the faollowing values of the range-finder parameters: $P_u = 1$ MW; $S_{onr} = 50 \, cm^2$; $\eta = 0{,}02$; $h = 2{,}8 \cdot 10^{-19}$ J; $\beta = 1$.

For a visibility range larger than 10 km, the range of the detection of the object is limited by the noise generated by the receiver, and by the noise caused by the background radiation. These noises were not taken into account when deriving formula (127) and constructing the graphs from Fig. 77.

Therefore, the range finder can work reliably only in the case of a high level of the received useful signal, i.e. the transmitted signals must have large power. To achieve high precision of the measurement of the distance, it is necessary that the time of the pulse growth be short; since only the front of the pulse is used, the pulse itself can be short. That is why in the pulse-type range finders lasers are used that generate especially short and powerful pulses of the optical radiation.

25. METHODS OF GENERATION OF SHORT-DURATION PULSES OF COHERENT OPTICAL RADIATION

To achieve the necessary precision and operating range of the optical range finders, their lasers must irradiate high-power, short-duration pulses, 10^{-7} to 10^{-9} s long. The usual pulse lasers are unsuitable for this purpose because pulses that short cannot be generated with the help of the lamps used at present for pumping.
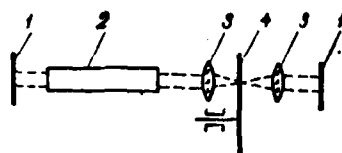
Fig. 78. Schematic diagram of an optical shutter with a rotating disk.

Short pulses can be obtained in lasers using resonators with controlled Q-factor that decrease the duration of the pulse by means of the accumulation of active atoms on a metastable level. This is achieved by an intentional decrease of resonator Q during the pumping pulse, as a result of which the conditions for self-excitation are not satisfied. After the termination of the pumping, when nearly all the active atoms are accumulated on the metastable level, normal Q of the resonator is quickly restored, and the excited atoms make a transition to a lower energy level, which results in a powerful pulse of optical radiation.

Devices used to control the resonator Q are called optical shutters. Active and passive optical shutters are distinguished.

The simplest construction of an optical shutter consists in a

rotating disk with a small opening, which is situated in the focal plane of telescopic system 3 (Fig. 78). Disk 4 interrupts the laser radiation in the region of the optical resonator 1, so that its Q is small and is determined by the reflection coefficient of the left mirror, by the free end of active substance 2, and by the non-mirror surface of the disk. When the radiation goes through the opening in the disk, the resonator Q increases sharply as a consequence of the reflection from the right mirror. A disadvantage of the described construction is a relatively long switching time (of the order of 10^{-6} s), and also destruction of the edges of the opening in the disk at high levels of the radiative power [16].

In   practice, one uses much more often active optical shutters with rotating prisms and mirrors. In the shutters of this type, one of the mirrors of the optical resonator rotates in such a way that the parallel position of the mirrors is achieved only in the course of a short time interval. As a rotating mirror, one can use any optical planes covered by a dielectric, or prisms with total internal reflection. It is expedient to use the prisms because they have the property of optical correction in the case of incorrect centering or incorrect adjustment of the bearings. It was determined experimentally that the output energy of the generator does not change more than by 20 % of its maximal value when the top of the prism is shifted relatively to the axis of the ruby bar within ±10 % of the diameter of the bar.

Because the laser with an optical shutter generates powerful radiation, which causes dammage to dielectric coatings of the
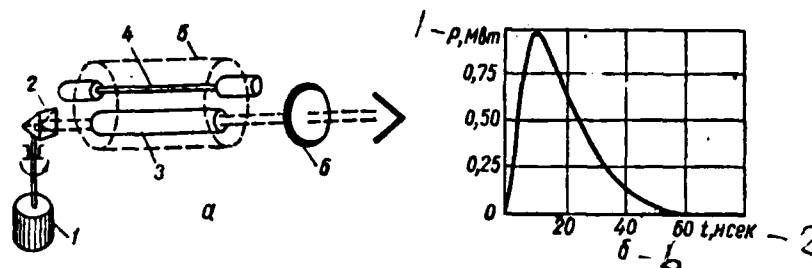
Fig. 79. Ruby laser with an optical shutter of the rotating-prism type.

1- P, MW; 2- t, nsec

ruby, one uses a separate mirror as the fixed reflector. To simplify its adjustment, this mirror is optically plane and is parallel to the end face of the crystal.

A simplified diagram of a ruby laser with an optical shutter is depicted in Fig. 79a. Polished ruby bar 3 is situated at one of the focal axes of elliptical reflector 5, at the second focal axis there is a mast-like pulse lamp 4. Front mirror 6 of the optical resonator is a glass, planparallel plate with a multi-layer dielectric coating having the reflection coefficient of 50 % for the wavelength of 0.6943 μm. Rear mirror 2 is a prism with total internal reflection. It is rotated by small motor 1 at the speed of 20,000-30,000 rev/min. At such speeds, the switching time of the resonator Q is approximately 10^{-7} sec. A small magnet situated in the prism holder and a magnetic receiver are used to determine the relative position of the prism and the moment of the beginning of the pumping pulse (duration 250 μs).

The form of one pulse generated by a laser with the described

optical shutter is shown in Fig. 79b. In a general case, the
pulse has approximately a triangular form. The asymmetry of the
pulse can be explained by an unsatisfactory frequency
characteristic of the photoconverter. When the distance between
the resonator mirrors is small, the period of pulse growth lasts
for 10 to 15 nsec, and the duration of the pulse at the level of
half power is $\Delta t \approx$ 20 nsec.

The quantity Δt can be determined by means of formula [16]

$$\Delta t = \frac{1 - \dfrac{\Delta_\kappa}{\Delta_0}}{v \sigma_{21}\Delta_0 \left[1 - \dfrac{\Delta_{nop}}{\Delta_n}\left(1 - \ln \dfrac{\Delta_{nop}}{\Delta_0}\right)\right]\dfrac{\Delta_{nop}}{\Delta_0}},$$

(128)

where Δ_0, Δ_k, and Δ_{nop} are initial, final, and treshold inverted
populations; σ_{21} is the cross-section of the stimulated radiation
of a quantum; v is the light velocity in the medium.

Using, for example, the values for ruby, $\Delta_0 = 0.8 \times 10^{19} \frac{1}{cm^3}$,
$\sigma_{21}\Delta_0 = 0.2 \frac{1}{cm}$, and $\frac{\Delta_{nop}}{\Delta_0} = 0.5,$ one obtains $\Delta t = 3 \times 10^{-9}$ sec,
which is in accordance with experimental data.

As follows from theoretical calculations, pulse duration does
not depend much on the rate of the change of resonator Q that is
determined by the speed of the prism rotation. Experimental
investigation indicates that this dependence is more pronounced.
Obviously, it is a consequence of the inhomegeneity of the
crystal and of the nonuniform conditions of its illumination
during the pumping, which results in nonuniform values of the
inverted population in various regions of the active medium,
thus these regions generate the radiation at different values of
the resonator Q.

48

The dependence of the pulse duration on the resonator length can be described by approximate relation [16]

$$\Delta t \approx \chi \cdot 10/(v\sigma_{21}\Delta_0) , \qquad (129)$$

where

$$\chi = (nl+L-1)/(nl) ;$$

l is the length of the active medium; L is the length of the resonator; n is the refraction index of the active medium.

For example, for ruby laser it is $\sigma_{21}\Delta_0 = 0.2 \frac{1}{cm}$, l = 5 cm, and L = 50 cm, which gives Δt = 18 nsec.

The speed of mirror rotation is a very important parameter of the generator with optical shutter. It was found experimentally that for a given pumping energy the number of generated pulses decreases with the increase of the speed of mirror rotation, and the pulse power increases considerably. The duration of a series of pulses is inversely proportional to the speed of rotation (see Table 21).

Table 21

Dependence of the parameters of the generated pulses on the mirror speed (pumping energy 200 J, inter-mirror distance 200 mm)

Mirror speed, 10^3 rev/min	Number of pulses	First-pulse power, MW	Second-pulse power, MW	Duration of a series of pulses, μsec
60	2	2.20	0.80	0.30
40	4	1.40	0.55	0.45
20	4	0.45	0.40	1
10	~8	0.25	0.25	2
5	~13	0.10	0.10	4

49

To increase the effective speed of mirror rotation, a laser with two mirrors is used (Fig. 80a). The effective speed of the mirror is then twice the actual speed (20,000 rev/min); however, the length of the optical resonator increases somewhat which results in narrowing of the generated beam and in the increase of the period of the pulse growth.
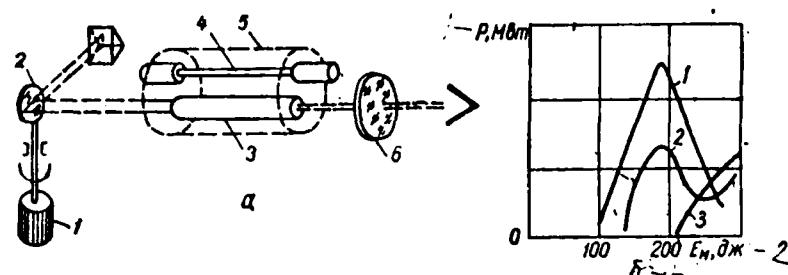

Fig. 80. Ruby laser with an optical shutter in the form of rotating mirror: a- schematic diagram; 1- servomotor; 2- rotating mirror; 3- ruby crystal; 4- pumping lamp; 5- reflector in the form of elliptical cylinder; 6- fixed (semitransparent) mirror; b- dependence of the pulse power on the pumping energy; 1- first pulse; 2- second pulse; 3- third pulse.

1- P, MW; 2- E_M, J

Let us investigate the dependence of the output power of the laser with a rotating mirror on the pumping energy and on the reflection coefficient of the fixed front mirror. In the experiments with ruby lasers it was found that the pulse output power increases up to a certain limit with the increase of pumping (Fig. 80b). For every pulse there is a threshold value of

pumping energy. The regime of the radiation of single pulses is possible only in a certain range of the pumping energies. If the pumping energy is less than the minimal energy of this range, the generator will not radiate at all; if the pumping energy lies above the maximal value, a series of pulses will appear.

Table 22

Dependence of the laser energy and of the output power on the reflection coefficient of the fixed mirror

Reflection coefficient, %	Energy, MJ	First-pulse power, MW
95	10	0.4
85	35	1.3
75	45	1.7
65	55	1.9
55	70	2.1
45	33	1.1
35	No radiation generated	

The influence of the fixed-mirror reflection coefficient on the laser energy and output power is presented in Table 22. Optimal reflection coefficient of the fixed mirror giving the maximal output energy of a laser with controlled Q can be determined from formula [16]

$$\rho_{2\,\text{опт}} = \exp\left[2l\left(\beta + \frac{\sigma_{21}\Delta_0 - \beta}{\ln\frac{\beta}{\sigma_{21}\Delta_0}}\right)\right],$$

(130)

where β is the coefficient of internal losses in the resonator.

E.g., for $\beta = 0.03\ \frac{1}{\text{cm}}$, $\sigma_{21}\Delta_0 = 0.2\ \frac{1}{\text{cm}}$, and $l = 5$ cm, one has $\rho_{2\,\text{опт}} = 0{,}55$.

51

The optimal value of the reflection coefficient depends on the initial level of inverted population, and varies with maximum output power and with maximum energy. This difference is especially significant in the case of small internal losses in the resonator.

The dependence of the output energy on the initial value of the inverted population and on the length of active medium is shown in Fig. 81. The output energy increases in a nonlinear way with the increase of the length of the medium.
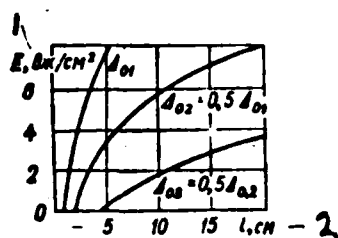

Fig. 81. The dependence of the output energy of a Q-switched laser on the initial value Δ_0 of inverted population and on the length of the active medium.

1- E, J/cm^2; 2- 1, cm

A characteristic parameter of the kinetics of the generation of short and powerful pulses is the time t_0 of the pulse development, which shows how rapidly appears a significant decrease of the population of the upper level when the resonator Q-factor has changed. Time t_0 depends on the size of the resonator, pumping level, and reflection coefficients of the system, and its typical value is 2×10^{-7} sec.

In the case of a slow switching on of the optical shutter, the laser irradiates a series of consecutive pulses (Table 21). During each pulse, the population inversion decreases to a value

smaller than the instantaneous value of the threshold at the
moment of the generation. The generation is interrupted until
the next stage of the process of switching on of the shutter when
the generation threshold is again lowered.

When the shutter is switched on rapidly so that no
oscillation can be initiated in the laser, all the energy stored
in the medium is irradiated in the form of one pulse. If a
rotating mirror is used as the optical shutter, even at the speed
of 30,000 rev/min the switching lasts approximately 1000 nsec,
which is much longer than t_0.

The speed of a mechanical shutter can be increased by means
of planparallel transparent plate as used in the Lummer-Gehrcke
interferometers. This plate functions as a one-dimensional
selector of the type of oscillations. Such an optical shutter is
depicted in Fig. 82. Beam a, for which the angle of incidence on
the lateral face of the plate equals the angle of total internal
reflection, goes through plate 3 without any damping. Beam b,
the angle of incidence of which is more sharp than that of beam
a, is damped along its course in the plate. Thus for the
deflection of 10^{-3} rad from the critical angle and for the plate
length corresponding to 10 reflections, the intensity of beam b
decreases approximately 10 times. Beam c, with the angle of
incidence larger than the critical one, returns, after the first
passage through the plate and after the reflection from mirror 4,
with an angle of incidence less the critical one, and thus dies
out in the same way as the beam b.

In this way, the reflective capability of the system

consisting of a planparallel plate and of a rotating mirror

depends on the angle of the mirror inclination, which enables one to

decrease considerably the switching time of the shutter without

increasing the speed of the mirror. To this end, the planparallel

plate is adjusted in such a way that the angle of incidence of

the axial beam on the lateral face of the plate exceeds somewhat

the critical angle. The time interval corresponding to the change

of reflection coefficient in the range of 10-100 % is determined

by the number of internal reflections, i.e. by the length of the
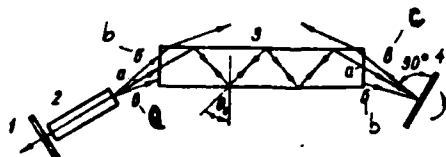
plate and the speed of the mirror.

Fig. 82. Schematic diagram of the optical shutter with a
planparallel plate: 1- output radiation; 2- laser; 3- planparal-
lel plate; 4- nontransparent rotating mirror (prism).

Experiments have shown that for the case of 12 reflections

during one passage of the beam along the plate, the reflection

coefficient changes in the range 1-100 % in the course of the

inclination by the angle of 0.2 μrad. For the mirror speed of

30,000 rev/min, this corresponds to the shutter switching time of

approximately 70 nsec.

Two modifications of this shutter are depicted in Fig. 83.

The main element of the shutter from Fig. 83a is planparallel

plate 2, in which the beam undergoes multiple reflections from faces c and d under angle of incidence near to the angle of total internal reflection. When the plate rotates around point O, its transmission changes, which can be used for the generation of powerful pulses of short duration. A similar shutter was tested in a neodymium laser with the diameter of 10 mm and the length of 120 mm. The resonator base was 500 mm. The planparallel plate, cut in such a way that eight reflections of the beam from its faces were observed in the case of a double passage through it, rotated with the speed of 24,000 rev/min. The length of the generated pulses was 35 nsec, which is half the pulse length for a similar scheme using a rotating prism [88].
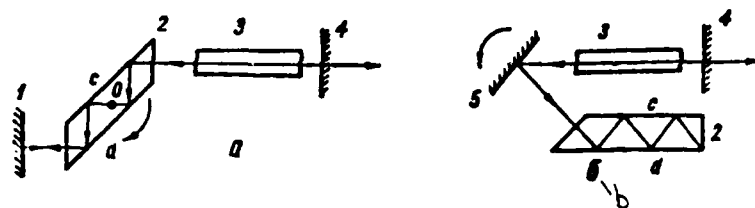

Fig. 83. Principle of optical shutters:
a- with a rotating plate; b- with a rotating mirror; 1- mirror; 2- planparallel plate; 3- active laser substance; 4- semi-transparent mirror; 5- rotating mirror (prism).

The second modification of the shutter is in Fig. 83b. In this case the planparallel plate is fixed, and the change of the angle of incidence on faces c and d is achieved by the rotation of the prism (mirror) 5. The function of the fixed mirror is

played by the end face of the plate, where total internal reflection occurs. Such shutter allows the use a laser with a large beam diameter because the planparallel plate is fixed and can have large size. Moreover, double pulses appear only at much higher pumping energies as compared with the shutter using one rotating prism.

Of other mechanical methods of Q switching, it is worth mentioning the one based on the change of the total light reflection from the surface of prism 2 when approached by dielectric plate 1 (Fig. 84a).

The coefficient of transmission of light through a layer between two dielectric media depends on the thickness of the layer. If the permitivities ϵ_1 and ϵ_2 of the dielectric media are larger than the permitivity of the layer between them, and the thickness d of this middle layer is much larger than the light wavelength, then the total internal reflection occurs for sufficiently large angles of incidence ϕ (Fig. 84b). The reflection coefficient decreases with the decrease of d, and for d=0 is given by Fresnel formulas for light reflection from the boundary of two media with dielectric permitivities ϵ_1 and ϵ_2.
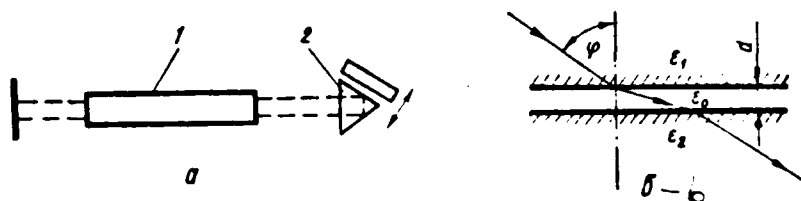

Fig. 84. Resonator Q-factor control by means of changing the conditions of the total internal reflection in the prism

In this way, one can change the Q-factor of the resonator by changing d by means of changing the position of the dielectric plate with respect to the reflective surface of the prism by one half of the wavelength. Mechanical shifting can be realized with the help of piezoelements [16].

Among active optical shutters, there also belong acoustical, electrooptical, and magnetooptical shutters. A laser with an ultrasound shutter is depicted in Fig. 85. Reflective surfaces of optical resonator 1 are adjusted so that no radiation is generated for the given level of pumping. Ultrasound cell 4 is situated between ruby crystal 9 and one of the reflective surfaces. If the light beam passes through the medium excited by vibration of a wavelength much larger than the width of the light beam, refraction occurs in the medium. This is used for the forming of high-power, short-duration laser pulses.

When the maximum excess population of the upper energy level is achieved, piezoelectric element of the ultrasound cell
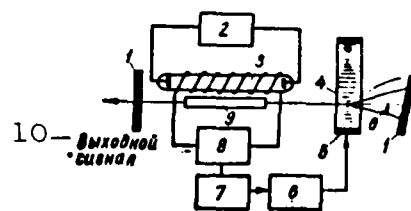

Fig. 85. Laser with an ultrasound refraction shutter: 1- optical resonator; 2- capacitor battery; 3- pumping lamp; 4- ultrasound cell; 5- piezoelement; 6- generator of sound vibrations; 7- time delay scheme; 8- trigger scheme; 9- ruby crystal.
10- Output signal

is instantly activated by a short voltage pulse, which results in sinusoidal variation of the refractive index of the medium. When the spontaneous radiation from the ruby bar passes through the utrasound field, the light beam starts to deviate periodically from the axis of the ruby bar, and during a short interval happens to be normal to the reflective surface of optical resonator 1. At the moment, the positive feedback is realized, i.e., the reflected beam falls on the end of the ruby bar, which gives rise to the stimulated emission and to the generation of a short pulse.

In one of the prototypes of the ultrasound shutter, the cell had the form of an parallelepiped with the base side equal to 64 mm, filled with alcohol. As the material of the exciter, one used the zirconate-titanate of lead. The resonance frequency of the exciter was 182 kHz. The triggering pulse of the exciter had the amplitude of 2400 V and the duration of 4μsec.

A laser with a ruby crystal 150 mm long and 6.4 mm in diameter was excited by two gas-discharge pumping lamps of the spiral type with the energy of 1800 J, placed in an eliptical reflecting system. Reflective coatings of the Fabry-Perrault resonator consisted of 13-layers of dielectric material, and had the reflection coefficients of 0.98 and 0.85 for the wavelength of 0.6943 μm. The distance between mirrors was 610 mm. For the registration of the laser radiation, a photomultiplier with filters was used. During the experiments, this laser generated pulses the amplitude of which was 50-70 times that of the pulses generated in the normal way. The pulse front was shifted by 2 to

2.5 μsec with respect to the moment of the flash of the pumping lamp. The power of the pulse was more than 1 MW; the duration of the growth of the pulse front was 30 nsec while the whole duration of the pulse was 75 nsec.

The switching time of electrooptical shutters is of the order of a few nanoseconds. The operation of such shutters is based on birefringence arising in liquids and in piezoelectric crystals as a consequence of the application of an external electric field.

Schematic diagram of an electrooptical shutter with one polarizer is shown in Fig. 86. Parameters of cell 2 are chosen in such a way that the phase shift for double passage equals π. Therefore, the shutter is open when there is no external field, and shut when the field is applied. There are also other constructions of electrooptical shutters in which the shut state corresponds to the absence of external fields.

As the material for electrooptical cells, nitrobenzol and KDR crystals are used most often. When using nitrobenzol and large power densities of the order of 10 MW/cm^2, the form of the pulses and the spectral character of radiation change considerably as a consequence of the stimulated Raman scattering and of parametric effects in the shutter material. Besides that, the transparency of nitrobenzol decreases in the course of the operation, and the collimation of the beam deteriorates because of optical inhomogeneities.

KDR crystals are more suitable because of high homogeneity of the crystal lattice and transparency in the range of up to 1.1 μm. A great advantage of those crystals is a low level of losses,
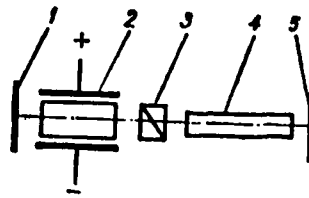
Fig. 86. Principle of the electrooptical shutter with one
polarizer: 1,5- optical resonator; 2 - electrooptical cell; 3- polarizer; 4- active medium
of the laser.

which precludes the possibility of their warming up during the

operation.

To create homogeneous electric fields, one uses circular

electrodes created by sputtering of gold on the surface of glass

plates glued to the polished surface of the crystal to protect it

from moisture dammage. A voltage of 8-16 kV is applied to the

electrodes.

One investigates also the possibility of using crystalline

quartz, which has linear transversal electrooptical effect [85],

in electrooptical shutters. If a quartz crystal is placed between

crossed polarizers, the dependence of transmission coefficient τ

of such system along axis Y on the voltage of electric fields

applied along axis X has the form

$$\tau = \sin^2\left[\frac{\pi d_Y (n_0 - n_e)}{\lambda} + \frac{\pi d_Y n_0^3 r_{11}}{2\lambda} E_x\right],$$

where d_Y is the dimension of the crystal in the direction of axis

Y; n_0 and n_e are refractive indexes of the normal and

60

extraordinary rays; r_{11} is electrooptical constant of quartz; E_x is electric field voltage along X-axis; and λ is the wavelength of the radiation passing through the system.

For $d_Y(n_0-n_e) = k\lambda$ (where $k=1,2,3, \ldots$) ,

$$\tau = \sin^2\left(\frac{\pi d_Y}{2\lambda} r_{11} n_0^3 E_x\right),$$

i.e., quartz crystal can be used as an optical shutter because transmission coefficient $\tau=0$ when control voltage $E_x=0$.

Electrooptical effect in quartz is approximately 20 times weaker than in KDR crystals, the consequence of which is a much larger dimension of quartz bars in the direction of Y-axis (around 100 mm). At the same time, the changes in temperature have an influence on the difference of paths of the normal and the extraordinary rays, which results in incomplete shutting of the shutter. To remove this disadvantage, one uses two identical quartz bars, the Y-axes of which have the same direction, and the axes X and Z of one of the crystals are perpendicular to the respective axes of the other one. If $E_x=0$, the difference of paths of the beams in the two crystals compensates mutually, not only for arbitrary wavelength, but also for diffferent temperatures.

The advantages of quartz in comparison with ADR and KDR crystals consist in broader pass band of transmitted radiation, in mechanical, thermal and chemical stability, in not being hydroscopic, and in simpler and more precise mechanical processing.

61

The experiments with the quartz electrooptical shutter were performed in an optical circuit consisting of quartz quarter-wave plate, control element in the form of two quartz bars each with the cross-section of 12x12 mm and the length of 100 mm, and a polarizer. The quartz bars were hermetically sealed in glass containers filled with refined transformer oil. As a polarizer, one used a prism of Iceland spar. It was found that by means of quartz electrooptical shutter one can obtain gigantic light pulses, stable in amplitude and duration. As regards the efficiency of the generation of gigantic pulses in a ruby laser, the quartz shutter is in many respects not worse than the electrooptical shutter using KDR crystals [85].

Optical shutters using the magnetooptical effect are used only in a limited extent because they have small switching speed and large losses in the control element. One of the best materials for this purpose is the dense flint glass, the maximum angle of rotation of which is 0.11 min/(deg/cm).

Recently, the development of passive optical shutters, based on the effect of increase of transparency of some substances under the influence of laser radiation, has been pursued intensively. If a passive medium with resonance losses is introduced into the resonator, the treshold level of pumping is increased, which results in the accumulation of active atoms on the metastable level. When the generation starts, the passage of the laser radiation through the passive medium sharply increases its transmission coefficient (Fig. 87), and the stored energy is irradiated in the form of a high-power pulse of the duration of
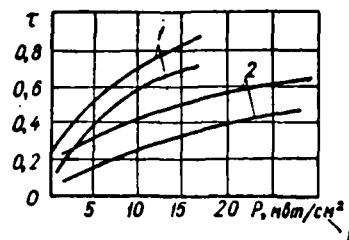
Fig. 87. Dependence of the transmission coefficient of passive medium of an optical shutter on the intensity of radiation passing through the medium: 1- solution of phthalocyanine in nitrobenzol; 2- solution of cryptocyanine in nitrobenzol.
1- P, MW/cm²

the order of 10^{-8} sec.

Absorbing dyes on a glass substrate and aluminized Mylar layer were used as passive media in the first experiments. However, because of their rapid destruction under the action of high-power pulses, one later started to use the solutions of phthalocyanines and cryptocyanines, polymethyl dyes in liquids and in plates, and also semiconductor materials.

In ruby lasers, one uses solutions of phthalocyanines and cryptocyanines of Mg^{2+}, Zn^{2+}, Ba^{2+}, and other metals. The solvents of phthalocynanines are nitrobenzol, toluol, and chlorbenzol; cryptocyanines are dissolved in methanol and ethyl alcohol. Phthalocynanine solutions are more stable than cryptocynanine ones. In the neodymium-glass laser, one uses solutions of polymethyl and organic dyes of the type of fluoresceine. The saturation in such absorbers takes place between two excited molecule levels, and not between the basic

63

and one of the excited levels as in other liquid passive media.

The use of passive shutters simplifies the laser construction, no synchronization mechanism is necessary, and one can achieve for the parameters of generated pulses the values approaching the limit ones, which correspond to the case of instantaneous Q-switching. Pulses of duration of only several picosecond have already been obtained. Such ultrashort pulses enable to realize optical range finders with the resolution less than 5×10^{-2} cm, and operating range of a few kilometers.

The schematic diagram of a device for the generation of ultrashort pulses is depicted in Fig. 88 [46]. Neodymium-glass laser 4 is the source of radiation. The laser resonator comprises cell 3 containing a saturated solution of an organic dye, electro-optical modulator 7, and polarizer 5. The cell with the organic dye changes the Q-factor of the resonator and plays the role of a shutter of passive type. The electrooptical modulator is filled with a transparent material that, being placed in the electro-optical field, acts as a high-speed switch of light flow. Initially, the modulator is in the unexcited state, and the polarizer is set to maximum transmission.

It is expedient to use the neodymium-glass laser for the generation of ultrashort pulses. The spectrum of its radiation consists of three lines broadened to 40 Å, partially overlapping each other, as a result of which a single line with nonuniform broadening up to 100 Å is created. In the case of the length of the glass bar of 185 mm, 8-nsec pulses with peak power of approx. 10^{11} W were successfully generated. In spite of
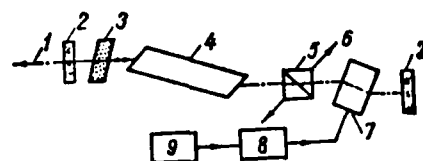
Fig. 88. Schematic diagram of the setup for the generation of ultrashort pulses. 1- output laser radiation; resonator mirror; 3- cell with an organic dye; 4- laser; 5- polarizer; 6- output signal; 7- electrooptical modulator; 8- pulse generator; 9- power supply.

the fact that at present there are no methods for the processing of such pulses, the perspectives of the use of optical systems with ultrashort pulses are very large because their resolution can be increased by several orders of magnitude with respect to that of radio range finders.

A peculiarity of passive shutters is the possibility of the selection of the types of oscillation, which results in the narrowing of the irradiated spectrum. This is explained by the fact that the threshold for various modes is not achieved simultaneously, but consecutively, as a function of the level of pumping. First, the high-Q modes are developed, corresponding to the center of luminescence. Their intensity most rapidly achieves such values for which the shutter is transparent, and an avalanche process of the pulse generation is started. In this way, the energy stored in the active medium is converted into the radiation of a few central modes [16]. With the help of passive shutters one can get a series of high-power pulses with a high

65

frequency of repetition. The interval between individual pulses is usually equal to several tens of microseconds, but it can be regulated by changing the energy of pumping and the absorption coefficient of the passive medium.

Optical shutters do not increase the energy of laser radiation. On the other hand, the total energy of coherent radiation that can be obtained with the given source of radiation decreases. However, the maximum power increases by several orders, and the duration and the form of pulses have the desired character, which is especially important in optical localization.

26. CONSTRUCTION OF OPTICAL RANGE FINDERS WITH PULSED AND CW LASERS

To illustrate the constructional solution of optical range finders working in the pulsed regime, let us inspect the most widespread foreign range finder "Colidar", developed by the American firm Hughes Aircraft.

It consists of transmitter, receiver, synchronizer, indicator, and the module for data processing. The receiver contains a ruby laser (ruby bar diameter is 10 mm, and its length 37 mm), an optical shutter, and an optical system decreasing the angular spread of the beam from 9 μrad (31') to 0.3 μrad (1.14').

The receiver consists of the optical part (a mirror telescope with the mirror diameter of 200 mm, interference filter with pass band of 13 Å), and the electrical part (photomultiplier with

66

cooling; amplifier). The optical part has the form of a
telescopic tube 250 mm long, on the axis of which the laser and a
telescope intended for the search of the target are mounted. The
signal from the load resistor of the photomultiplier is amplified
by means of a two-stage amplifier. The first stage uses
transistors, and its voltage gain equals 100 and its output
resistance is 200 Ω.

The range finder indicator is a two ray oscillograph on the
screen of which the reference and the reflected pulses are
displayed. The scan of both signals is synchronized by the pulses
from the transmitter. The distance to the target is determined
from the time lapse between the reference and the reflected
signal. The synchronizer serves for creating a reference signal at the moment
of start-up of the oscillator. The synchronizing pulse is obtained on the case of
selection of a negligible part of the laser radiation. To this end, a sparse
wire grid is situated behind the collimator. The radiation
reflected by the grid is concentrated with the help of a lens on
the photomultiplier photocathode. After preliminary
amplification, the output signal of the photomultiplier is led
to the indicator to trigger the scan, and to the amplifier of the
vertical deviation of the second beam.

The resolution of "Colidar" is very large. On a clear day, at
the distance of 100 km, one can distinguish two stationary
objects of grey color separated one from another by 3 m.

According to a similar blueprint, a portable range finder
intended for a precise measurement of distance within the range
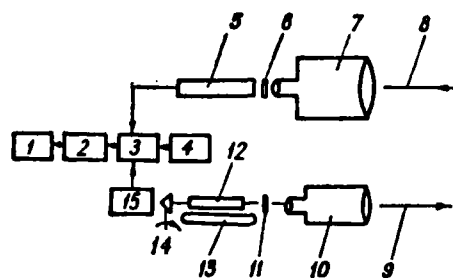of 10 km was built [52]. Active laser medium is a ruby rod 76 mm

Fig. 89. Functional diagram of an optical range finder with ruby laser: 1- range indicater; 2- pulse counter; 3- stroboscopic cascade; 4- pulsed generator; 5- photomultiplier; 6- optical filter; 7- objective; 8- reflected signal; 9- laser radiation; 10- collimating system; 11- fixed semi-transparent mirror; 12- ruby; 13- pumping lamp; 14- rotating prism; 15- photodiode.

long and 6.35 mm in diameter, placed on one focal axis of an elliptical reflector. On the second axis, there is the pumping lamp. The optical shutter consists of a prism rotating with the velocity of 15,000 rev/min. The switching of the Q-factor of the optical resonator sets in the laser the regime of the generation of high-power pulses of the duration of 40 nsec. The width of the irradiated line is 0.1 Å, its wavelength 0.6943 μm, and the power in a pulse is 4 MW. The degree of collimation is estimated to be 0.5 μrad, which corresponds to the spot diameter of 0.5 m at the distance of 1 km.

Functional diagram of this range finder is in Fig. 89. The release of energy stored in ruby 12, and its irradiation in the form of a pulse occurs at the moment when the face of rotating prism 14 is parallel to semi-transparent mirror 11 of the optical

resonator. The largest part of the laser radiation is led through the prism into photodiode 15, the output signal of which is amplified and led to stroboscopic cascade 3, opening it.

The stroboscopic cascade is closed by the pulse reflected from the object the distance of which is being measured. Reflected signal 8 is received by optical system 7, and proceeds through filter 6 to the photocathode of the photomultiplier 5. The optical filter, with the pass band of 20 Å and 65 % transparency, limits background radiation. Distance reading is performed by pulse counter 4 having the frequency of 30 MHz. The generator is connected to the stroboscopic cascade.

With the pulse power of 4 MW and under medium weather conditions, the operating range of this range finder is 6 km, and under good weather conditions, it is 10 km. The weight of the device is 15 kg; power is supplied from batteries that are sufficient for 75 "shots"; maximum frequency of pulse repetition is 1 pulse in 10 sec; maximum error in the measurement of distance is 5 m.

In spite of the fact that the peak power of solid lasers is of the order of megawatts, their use in optical locators is aggravated by the low repetition frequency. The latest development of range finders abroad is connected with the use of semiconductor and gaseous lasers.

Let us discuss the construction of an optical range finder with a semiconductor pulsed laser. The advantages of the GaAs laser with the wavelength of 0.840-0.900 μm are:
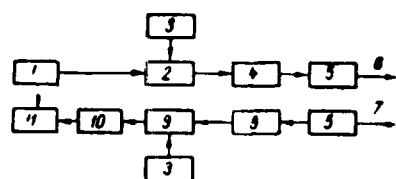
1) very small weight and size; 2) large efficiency

Fig. 90. Functional diagram of an optical range finder with semiconductor laser: 1- trigger generator; 2- modulator; 3- power supply ; 4- laser; 5- optical system; 6- irradiated signal; 7- reflected signal; 8- integrating filter; 9- photomultiplier; 10- coincidence filter; 11- oscillograph.

coefficient; 3) ability to work at room temperature; 4) the possibility of direct modulation by short pulses or high-frequency oscillations.

Compared to solid lasers, semiconductor lasers have small peak power (in the range of 10-100 W), which allows the measurement of relatively small distances.

The functional diagram of such range finder is shown in Fig. 90 [51]. Its main element is a semiconductor laser situated in a Dewar container and working at the temperature of 77 K. The laser is excited by current pulses of the amplitude of 40 A, duration of 100 nsec, and repetition frequency of 330 Hz; the generated peak power is 9 W, irradiated wavelength $\lambda=0.844$ μm.

The pumping current pulses are formed by means of a modulator realized as an artificial long line with concentrated parameters. Its schematic diagram can be found in Fig. 91. The delay line consists of a five-fold LC-circuit with the characteristic
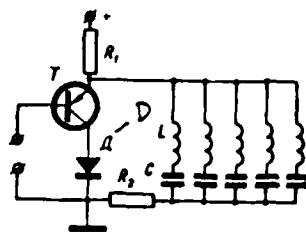
Fig. 91. Schematic diagram of the modulator of an optical range
finder

impedance of 4 Ω; as the discharge switch, one uses p-n-p-n
transistor T. In the series with the line and with semiconductor
diode D, resistor R_2 of 4 Ω is connected for impedance matching.

Laser radiation goes through a glass window in the Dewar
container and is collimated with the objective 45 mm in diameter
with focal length of 90 mm. The objective forms a beam of angular
width of 0.4x0.8 μrad; solid angle of the beam divergence is
3.2×10^{-7} sr. In the receiving optical system, one uses an
objective of the diameter of 140 mm and focal length of 508 mm.
As the photoconvertor, one uses the photomultiplier with
sensitive layer S-1; darkness current of the photomultiplier at
room temperature equals 10^{-13} A, quantum efficiency 3×10^{-3}. The
solid angle of the viewing field of the optical system is
3.8×10^{-5} sr.

To decrease the influence of the background radiation, one
uses an interference filter with pass band of 76 $\overset{\circ}{A}$ at the
wavelength of 0.844 μm; its transmission coefficient in the
center of the line equals 0.42 at +21 °C, and 0.31 at -17.6 °C.

Maximum operation ranges of the range finder in the condition

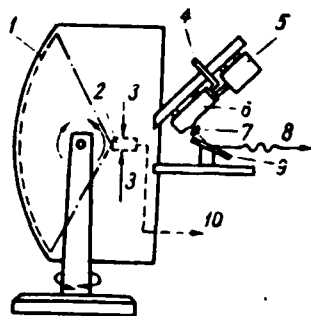| Fig. 92. Transmitter of the | Fig. 93. Transmitter of the |
optical range finder for the	optical range finder with
measurement of the cloud height:	an semiconductor laser: 1-
1- mirror objective; 2-	power supply (6 kV, 100 μA);
photomultiplier; 3- high-voltage	2- loosening resistor; 3-
power supply of the photo-	pulse generator on a Cu plate;
multiplier; 4- coaxial line for	4- moving electrode; 5- coax-
the measurement of current	ial line; 6- GaAs; 7- Dewar
pulses; 5- generator of the	container; 8- measuring coax-
current pulses; 6- Dewar	ial line; 9- input of sound
container; 7- lens; 8- radiation	modulation signal; 10- pulsed
(λ=0.84 μm); 9- mirror declined	signals (amplitude 50 V,
by 22.5 °; 10- line to the	duration 10 μsec, frequency
videoamplifier and oscillograph.	50 Hz).

of good visibility for various objects are: for trees, 235 m; for trees on the side of a hill, 268 m; for telephone poles, 95 m; for white-color buildings, 235 m; for concrete buildings, 265 m; for an hangar of corrugated metallic sheets, 2060 m.

Let us discuss another construction of a range finder with

semiconductor laser, intended for the measurement of the height

of clouds. Its transmitter part is depicted in Fig. 92. Its main

element is a GaAs semiconductor generator of optical radiation.

The diode is submersed in a hermetically sealed Dewar �6container

filled with liquid nitrogen. The diode is fed with pulses with

peak current value of 200 A, repetition frequency of 50 Hz,

duration of 30 nsec, and front duration of 5 nsec. The generated

beam is focused by lens 7. The measured peak power of the

irradiated signal is 100 W.

One of the difficult problems encountered when developing

optical range finders with a semiconductor laser is the

construction of the generator of short pulses for the modulation

of the diode radiation. The output impedance of the generator

must be in agreement with the very low impedance of the diode

(0.1 Ω). To this end, one uses coaxial line 4 with wave impedance

of 50 Ω. The impedance matching is ensured by the resistor of

1 Ω attached in series with the diode. This resistor serves also

for the measurement of current flowing through the diode.

The pulse generator uses a RC-circuit switched by a trigger

tube with a cold cathode (Fig. 93). As the storage element, one

uses a small-inductance capacitor that can be charged through a

large resistor to the voltage of 3.6 kV. When the tube opens, the

capacitor is discharged through the diode connected to the

generator by means of coaxial line 5 with the wave impedance of

1 Ω. Generator 3 is attached to the cover of the Dewar container

7. Through the cover goes coaxial line 5 and measuring coaxial

line 8 with wave impedance of 50 Ω. The lines are manufactured
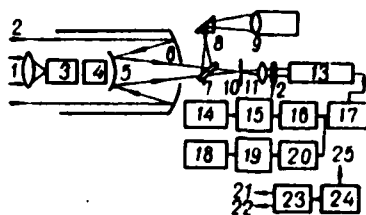
73

Fig. 94. Functional diagram of an optical range finder with high-power GaAs laser: 1- collimated laser radiation; 2- radiation reflected from the object; 3- semiconductor laser; 4- modulator; 5- secondary mirror of the receiving optical system; 6- primary mirror; 7- semi-transparent mirror; 8- prism; 9- optical pointing; 10- diaphragm; 11- lens; 12- narrow band filter; 13- photomultiplier; 14- distance indicator; 15- digital counter; 16- threshold circuit; 17- preamplifier; 18- distance indicator; 19- analog counter; 20- threshold circuit; 21- to photomultiplier; 22- to modulator; 23- voltage convertor; 24- power supply; 25- to electron circuit.

of thin-wall Cu-Ni pipes. The receiving part of the range finder consists of 1.5-meter parabolic reflector 1 with focal length of 66 cm, photomultiplier 2, situated in its focus, and broadband amplifier. The sensitivity of the photomultiplier is 400 μA/W, and its restoring time 2 nsec.

Experimental optical range finders with a semiconductor laser work reliably for distances up to 500-600 m.

Optical range finder from Fig. 94 belongs among the latest developments. The source of the optical radiation is a high-power GaAs laser having the following parameters: output power of 100

74

W; working current of 600 A; radiating area, 3x500 μm; angular divergence of the beam, 20x20 degree; repetition frequency, 1000 pulses/sec; efficiency coefficient of 15 %. The diode has a radiator ensuring a homogeneous current distribution, and an external mirror to reflect the radiation from one of the ends of the junction. The spectral width of the radiation lies in the range of 10-20 Å; the shift of the wavelength caused by temperature change is approx. 1.75 Å/deg. With the help of a collimating lens, the angular divergence of the radiation, Ω_{col}, decreases to 2 μrad because in that case

$$\Omega_{\text{кол}} = \frac{l}{f}.$$

where l is the width of the radiating area (p-n-junction) and f is the focal length of the collimating lens.

Laser pumping is done by a small pulse generator (Fig. 95). The principle of its work consists in charging the capacitor to the required voltage, and then discharging it through the diode connected in series with a tube with cold cathode. Internal resistance of the diode is 0.2 Ω. The resistor connected in series with the diode controls the parameters of the pulse with the help of an oscillograph. This resistor consists of ten resistors connected in parallel to decrease the self-inductance.

The energy is accumulated in capacitor C_1. If $R_1 C_1 \ll R_2 C_2$, the pulse repetition frequency is determined by time constant $\tau = R_2 C_2$. A change in voltage U influences the pulse amplitude and the frequency of pulse repetition. The time of the pulse growth
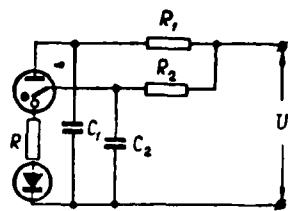
75

Fig. 95. Schematic diagram of a small pulse generator intended for laser pumping.

equals approximately 15 nsec.

GaAs diode and collimating lens are placed in a common brass case situated in front of the secondary mirror of the receiver (Fig. 94).

Reflected radiation is being received by the mirror system with focal length of 500 mm and aperture area of 100 cm². The radiation is focused on a diaphragm of the diameter of 2.5 mm (limiting the viewing field of the system), and is further directed to a simple spherical lens, with the help of which a beam of parallel rays arrives upon an interferential narrow-band filter. The focal length of the lens is 20 mm; width of the pass band of the filter is 100 Å; transmission coefficient for the wavelength of 0.902 μm is about 60 %.

Behind the spectral filter there is a photomultiplier with the photocathode of the type S-1. Quantum efficiency of the photocathode for the wavelength of 0.902 μm equals 3×10^{-3}. Photomultiplier is enclosed in a metallic case together with voltage divider, interferential filter, lens, diaphragm, and semitransparent mirror necessary for the operation of the optical finder. The mirror has a large transmission coefficient in the

76

infrared region of the spectrum and a large reflection coefficient in the visible part of the spectrum.

The videoamplifier on the output of the photomultiplier has three stages using transistors. Its total gain is 55 dB and its band width 40 MHz. The amplified photomultiplier signal is led to the digital and analog evaluator. Output from the digital evaluator is led to a digital indicator, which shows the distance every second. The data on the digital display are remembered till the next measurement of distance, which is suitable for the determination of the distance of fixed or slowly moving objects.

Analog evaluator measures the distance continuously; the distance is indicated by the deviation of an arrow or automatically plotted.

Schematic diagram of the analog evaluator is shown in Fig. 96. Trigger pulse 1 is generated by means of voltage change on the injecting diode, and the stop pulse 4 by the photomultiplier signal if it exceeds the level previously set by the treshold circuit 5. Trigger and stop pulses are led to bistable multivibrator 6 transforming the two pulses in one, the length of which equals the time interval between the trigger and the stop pulses. Rectangular pulse of length t is led through amplifier 7 to integrating RC-circuit 10. The time constant of this circuit is large compared with time interval t; that is why one can assume that the capacitor voltage increases linearly with the increase of the pulse length. From the integrating circuit the voltage is led to amplifier 13 with high output resistance, and
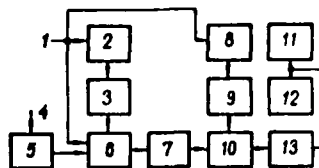
77

Fig. 96. Schematic diagram of an analog evaluator of distance

further to arrow indicator 11 or plotter 12.

If the time interval between two consecutive trigger pulses is less than the time constant of the device, pulse averaging occurs. Prior to the new series of the trigger and stop pulses, the capacitor is fully discharged by means of two waiting multivibrators 8 and 9, and a switching transistor. If the amplitude of the reflected signal is less than a preset level, the waiting multivibrators 2 and 3 return multivibrator 6 to its initial state.

Schematic diagram of the digital evaluator is in Fig. 97. Trigger pulse 1 is led through threshold circuit 2 to bistable multivibrator 4 together with stop pulse 5. On the output of the multivibrator a rectangular pulse, the duration of which is proportional to the distance to the object, appears. This pulse starts coincidence circuit 9, on the input of which there is also the voltage with frequency of 15 MHz generated by generator 10 with quartz stabilization (frequency of 15 MHz corresponds to distance resolution of 10 m). The pulses of clock generator are measured by three-stage counting circuit 6 on the output of which there is decipherer 8 with an electromagnetic relay. The measured distance is indicated by digital indicator 7. When
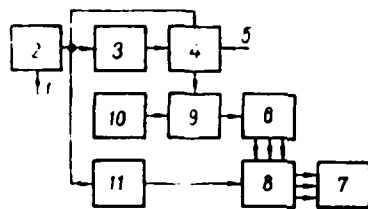
78

Fig. 97. Schematic diagram of a digital evaluator of distance

turned on, the counter is automatically set to zero by returning
circuit 11. Returning circuit can also be started manually.

The maximum delay of the distance strobe is ensured by
waiting multivibrator 3, which is started by trigger pulse and
generates the delay pulse of the duration of 6 μsec,
corresponding to the distance of 914 m. This pulse switches
multivibrator 4 when there is no signal reflected from the
target.

The length of the locator is 380 mm, diameter 75 mm, and
weight 4 kg. The volume occupied by the anolog evaluator (without
the indicator) is 65.6 cm^3. The dimensions of the digital
evaluator without the indicator are 125x90x30 mm. The power
consumption (without the digital indicator) is 1.8 W (voltage 12
V, current 150 μA). The error of the device is 5 % +0.9 m.
Angular resolution is 5 mrad.

For the theoretical calculation of maximum operating range
D_{max} of the locator, the transmission coefficient of the
atmosphere is determined by means of the formula

$$\tau_a = \exp(-\sigma D_{max}) \ ,$$

79

where σ is damping coefficient per unit length of the laser beam path.

The dependence of σ coefficient on the visibility range is shown in Fig. 98. The reflection coefficient of the background radiation was taken from the graph in Fig. 99.

To obtain a high precision of the distance measurement, one started to use CW gas lasers and the method of phase comparison of HF signals. To measure the distance with precision not exceeding 5 m, the required time resolution must be less than 20 nsec, which is the limiting value for systems working in the pulse regime.

The disadvantage of the phase method connected to the ambiguity in the measurement of distance can easily be removed by measuring phase shift simultaneously for several frequencies. In this case, the ambiguity is resolved if for each frequency one knows the phase shift corresponding to the time the signal needs to get to the target and back. In the case of moving targets, one has to take into account Doppler effect when calculating the distance.

If the phase difference between the transmitted and received signal is equal to zero, an integer number of halfwaves matches distance D. This condition can be mathematically expressed by means of the formula:

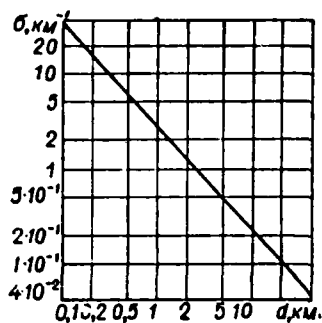$$D = n\lambda/2 = nc/2f \ , \tag{131}$$

where $n = 1, 2, 3, \ldots$.

Fig. 98. Dependence of the
coefficient of the damping of
radiation in the atmosphere
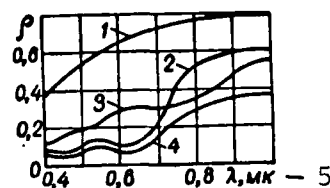on the visibility range
(λ=0.9 μm).

Fig. 99. Spectral coefficient of
radiation reflection for various
natural formations: 1- limestone,
alumina; 2- deciduous forests in
summer and green grass; 3- sand;
4- coniferous forests in summer,
dry meadows and grass; 5 - microns

For two frequencies satisfying condition (131), one can write

$$D = n_1 c/2f_1 \; ; \; D = n_2 c/2f_2 \; .$$

Therefore,

$$D = mc/2(f_2 - f_1) = mc/2\Delta f \; , \tag{132}$$

where m is the number of intervals between phase shift zeros when
the frequency changes continuously from f_1 to f_2.

If Δf is held constant, m will be proportional to distance.
In practice, one counts not m, but the number of phase shift
zeros, N, when frequency changes from f_1 to f_2; it is m=N-1.

To measure the distance with large precision, it is
necessary, besides the integer number of intervals between zero
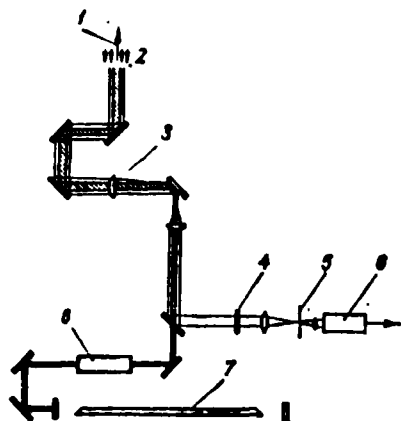points, to measure also fractional parts of these intervals. If

Fig. 100. Optical diagram of a range finder with CW laser: 1- ir-
radiated signal; 2- reflected signal; 3- objective; 4- optical
filter; 5- diaphragm; 6- photomultiplier; 7- gas laser; 8-
electrooptical modulator.

the magnitude of the error is supposed to be 1 m at the distance
of 10 km with Δf=10 MHz, the value of m must be measured with the
precision of 1/32 of the interval between the zero points of
phase shift. To measure the fractional part, it is necessary to
perform the frequency modulation of the signal according to a
special law.

Finally, we will discuss the optical circuits of a locator
[55] using a CW laser (Fig. 100). As the source of radiation,
He-Ne laser 7 with the power of 50 MW, working on the wavelength
λ=0.6328 μm, is used. The output signal goes through electro-
magnetic modulator 8 and optical system 3, and is irradiated in
the direction of the object the distance of which is being
measured. The width of the beam equals 1 mrad. The signal
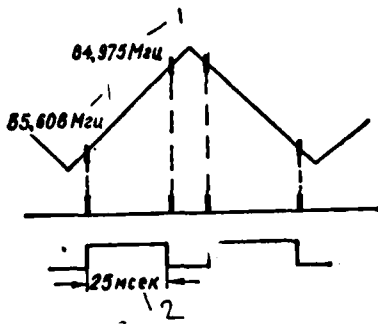reflected from the object goes through filter 4 with the pass

82

Fig. 101. Law of frequency modulation and the form of the main stroboscopic pulse.
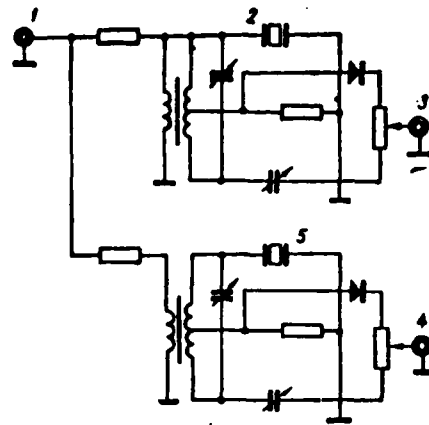1- MHz; 2- μsec

Fig. 102. Schematic diagram of the generator of control signals (frequency marks): 1- signal from the swinging frequency generator; 2 and 5 - quartz crystals; 3- signal of the frequency of 55.606 MHz; 4- signal of the frequency of 64.975 MHz.

band of 10 Å, cutting off the background radiation, and is directed to photomultiplier 6 with photocathode S-20. Output signal proceeds to the circuit of distance evaluation.

Laser radiation is modulated by means of an eloctrooptical modulator consisting of two ADR crystals 12.7 mm in diameter, which are supplied with modulating voltage from a swinging frequency generator. Its frequency is changed in a mechanical way, with the help of an electric motor driving the rotor of a capacitor. The form of the rotor is such that a triangular frequency dependence (Fig. 101) is obtained. $\Delta f=9.369$ MHz, which gives $c/2\Delta f=16$ m.

The main stroboscopic counting pulse is triggered and stopped

by signals generated by the balanced bridge circuit using quartz crystals 2 and 5 with the frequencies of 64.975 and 55.606 MHz, respectively. The circuit is balanced for all frequencies except the frequencies for mark monitoring (Fig. 102). The signal of variable frequency generated by the photomultiplier is led to the amplifier with the central amplified frequency of 60 MHz, and then proceeds to a phase detector working also in the region of 60 MHz. Simultaneously, also the reference signal, which is the attenuated signal from the generator of swinging frequency, is brought to the phase detector. The output pulses from the phase detector, corresponding to the zeros of phase shift, are amplified and brought to the evaluator.

The effect of the Doppler frequency shift, that could be a potential source of errors, is eliminated by averaging the values of distance measured during the increases and decreases of swinging frequency. The magnitudes of Doppler shifts during these periods are equal, but of opposite sign, that is why the averaging will eliminate the effect of Doppler shift [55].

During the testing of the described system, the error of ±1 m in the range distances of 300 m to 10 km was obtained. The maximum range of operation is determined by the irradiated power and by atmospheric conditions. The minimum operation range is not limited by the principle of the function of the system and can be considered to be zero.

An optical distance finder working together with a reflector placed on the object has somewhat different construction. In the daylight in clear atmosphere with He-Ne 100 MW laser with the
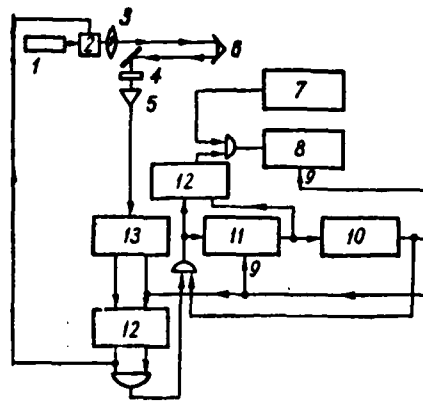
Fig. 103. Functional diagram of a range finder: 1- laser;
2- modulator; 3- lens; 4- photoconvertor; 5- preamplifier; 6-
reflector; 7- pulse generator; 8- decimal distance counter; 9-
trigger pulse; 10- multivibrator; 11- binary counter; 12-
trigger; 13- formation circuit.

beam divergence of 1.5 μrad, it is possible to obtain
sufficiently strong reflected signals from a reflector of an area
of 10 cm^2 at the distance of 30 km [32].

The system of distance evaluation operates in the digital
regime and yields data at the rate of 200 1/sec. The source of
radiation is a He-Ne laser with wavelength of 0.6328 μm. Plane-
polarized laser radiation is modulated by a rectangular wave, the
period of which is determined by the time of propagation of the
radiation to the object and back. Measuring the frequency of
modulation, one can determine the distance to the object.

Schematic diagram of the locator is shown in Fig. 103. At the
moment t=0, modulator 2 is switched on. After the interval
$t_1 = 2D/c$, the reflected signal arrives at convertor 4, and then

85

after the delay time t_0 the front of the reflected signal starts trigger 12, which switches off the modulator. From the time of the switching on of the modulator until the moment $t_2 = 2(2D/c+t_0)$, the reflected radiation arrives at the photoconvertor. At the end of this period the modulator is switched on again, and the described process is repeated.

The length of the reflected signal is measured by the number of signals generated by the external stable pulse generator, electronic clock 7, working at the frequency of 10 MHz. Electronic clock is started by the front of the working signal, and is stopped by its end. The number of pulses, proportional to the distance of the object, is counted by the distance evaluator.

The distance of the target is determined from the following equations:

$$N = (2D/c+t_0)\, Mf_0\ ; \tag{133}$$

$$M = [S(2D/c+t_0)]^{-1}\ . \tag{134}$$

From (133):

$$D = Nc/(2f_0 M) - ct_0/2\ ,$$

which gives

$$\Delta D \approx (\partial D/\partial N)\Delta N + (\partial D/\partial f_0)\Delta f_0 + (\partial D/\partial t_0)\Delta t_0 + (\partial D/\partial c)\Delta c\ . \tag{135}$$

If the synchronization and the phase comparison of the pulses of the electronic clock with the laser signal are not provided, then $\Delta N=1$. If $D>1000$ m and $t_0 \simeq 10^{-6}$ sec, it is $D \gg \frac{c}{2}t_0$. After some transformation, one gets for the repetition frequency of 200 sec^{-1} the formula

$$\Delta D = 200D/f_0 - D\Delta f_0/f_0 - \frac{c}{2}\Delta t_0 + D\Delta fc/c .$$

For the frequency generated by the electronic clock, 10 MHz, and for the distances larger than 300 m, the main element determining the error in the measurement of the distance seems to be $200D/f_0 = 2 \times 10^{-5}$ D . E.g., for the distance of 30 km, the error is $\Delta D \approx 0.6$ m.

Foreign firms work hard on optical range finders for the determination of the coordinates of submarine objects. The main difficulties in this case are connected with large absorption of radiation in water. Experiments show that the damping coefficient of coherent radiation in sea water changes in a wide range of values and depends on the wavelength. The lowest value of this coefficient corresponds to wavelengths from the blue-green part of the spectrum. Radiation of lasers with ionized argon with wavelength of 0.4579, 0.4658, 0.4765, 0.4888, and 0.4960 μm is only weakly absorbed in salt or fresh waters.

The approximate expression for the range of signal transmission has the form:
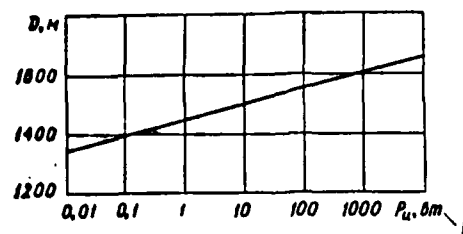
87

Fig. 104. Graph of the dependence of the penetration depth of the coherent radiation into the salt water upon the power of the radiation.

1 - W

$$D = -\frac{2.3}{a} \lg \frac{3P_{m}}{P_{u}} \quad [\text{meters}] \quad (136)$$

where a is the damping coefficient, m^{-1}; P_{m} —is the equivalent power of the receiver noise, W; P_{u} —is the power of the laser radiation, W.

Transmission coefficient of sea water for $\lambda = 0.47$ μm has the value of 0.97 m^{-1}. The graph of the dependence of the penetration depth of coherent radiation into salt water is shown in Fig 104 [81].

The main data on the optical range finders of foreign provenience are given in Table 23. When analyzing these data, it is necessary to take into account that the constructions of these locators are experimental and their parameters are taken from the publications in foreign journals that often have advertising character.

88

Table 23

Main parameters of the optical range finders of foreign origin

/— Тип дальномера (фирма, разработчик)	2— Тип генератора	3 — Передатчик		
		4 Ширина луча, м/рад	Частота повторения импульсов, имп/мин	6 Мощность в импульсе, квт
«Colidar», Hughes Aircraft	/2-ОКГ на рубине (d = 10 мм, l = 37 мм)	0,3	60	10
«Colidar» Marc II Hughes Aircraft	ОКГ на рубине -/2	0,2	3	1000
Martin	/2-ОКГ на рубине (d = 6 мм, l = 50 мм)	1,5—2	2	100
Raytheon	ОКГ на рубине -/2	—	6	100—1000
«Хе—6» RCA	—	—	4	1000
North American Aviation	—	—	6—10	5000
ХМ-23 (США) 2а	ОКГ на рубине -/2	—	10	3000
2 — Станфордский научно-исследовательский институт (США)	ОКГ на рубине -/2 (d = 63,0 мм, l = 75 мм)	0,5	6	7000
2о — Центральная лаборатория телесвязи (Франция)	ОКГ на рубине -/2	0,5	3	1000

7 — Приемник	8 — Дальность действия, км	9 — Точность измерения, м	10 — Вес, кг	11 — Примечание
13 — Зеркальный объектив, фильтр (13Å), фотоумножитель	10	10	14	14 — Длина оптического ствола 950 мм
15 — Объектив (d = 50 мм), фотоумножитель	12—15	4,5	19,8	16 — Источник питания — кадмиево-никелевые аккумуляторы. В условиях дождя дальность действия не превышает 5 км
17 — Объектив (d = 120 мм, f = 340 мм), фильтр (10Å), фотоумножитель	10	10—15	27	Объем 43 дм³ — 18
—	8	3—6	10	Полевой портативный прибор. Длина оптических стволов 500 мм — 19
—	5	10	13,5	Полевой портативный прибор — 20
—	16—25	0,3—10	11,5	Портативный прибор модульной конструкции — 21
22 — Зеркальный объектив, фильтр (10Å), ФЭУ	3—5	2,5	11,5	Источник питания — две никель-кадмиевые батареи — 23
25 — Объектив (d = 100 мм, f = 600 мм), фильтр (20Å), ФЭУ	6—8	5	25	—
27 — Объектив площадью 50 см², фильтр (40Å), ФЭУ	7	±2,5	40	Питание от источника переменного тока 50 гц или батареи 24 в — 24

1- Type of the range finder (manufacturer, developer); 2- Type of the laser; 3- Transmitter; 4- Beam width, m/rad; 5- Frequency of pulse repetition, min^{-1}; 6- Power in the pulse, kW; 7- Receiver; 8- Operation range, km; 9- Precision of measurement, m; 10- Weight, kg; 11- Note; 12- ruby laser; 13- Mirror objective, filter (13 Å), photomultiplier; 14- The length of optical barrel: 950 mm; 15- Objective (d=50 mm), photomultiplier; 16- Power supply: Cd-Ni accumulators. In the rain, the operation range does not exceed 5 km; 17- Objective (d=120 mm, f=340 mm), filter (10 Å), photomultiplier; 18- Volume: 43 dm^3; 19- Portable field device. The length of optical barrels: 500 mm; 20- Portable field device; 21- Portable device with modular construction; 22- Mirror objective, filter (10 Å), photo-multiplier; 23- Power supply: two Cd-Ni accumulators; 24- Stanford Research Institute (USA); 25- Objective (d=100 mm, f=340 mm), filter (20 Å), photomultiplier; 26- Central laboratory for telecommunications (France); 27- Objective with the area of 50 cm^2, filter (40 Å), photomultiplier; 28- Power supply: either ac current, or a 24 V battery; 29- USA

27. SYSTEM OF AUTOMATIC TRACKING OF MOVING OBJECTS

The purpose of the system of automatic tracking is to get continuous information on the position of a moving object. The obtained information can also contain data on the angular velocity of the moving object and on the distance between the object and the point of observation.

Because of small magnitude of the working wavelength, the precision and the resolution of optical systems of tracking of moving objects are much larger than those of the similar radiolocator systems. Because of the same reason, the diameter of the receiving objectives of optical systems is much smaller than the diameter of radiolocator antennas. Directional diagram of an optical system does not contain the side loops, which enables to exclude the false reflections. As well reflections from the Earth surface are excluded.

Compared with the passive system of tracking using the thermal radiation of the objects, an active laser system has better selectivity, and, beside that, enables one to measure the distance of the object and its speed.

Especially large attention to high-precision systems of automatic tracking of moving objects was given in connection with the necessity to equip polygons and testing sites with tracking eqipment, and also with the problem of the encounter of spaceships, and with the realization of the system of long-range optical communication using narrow beams.

First systems of automatic tracking used crystalline lasers

MICROCOPY CHART
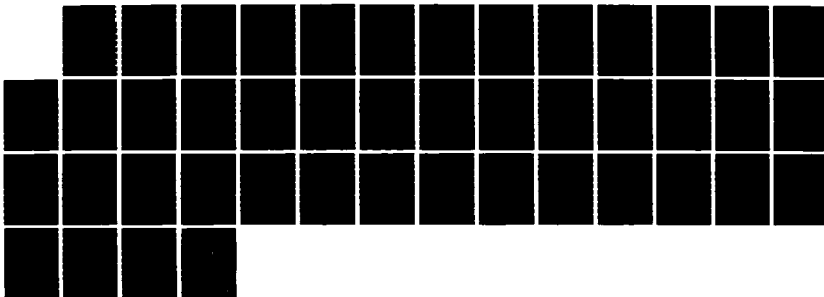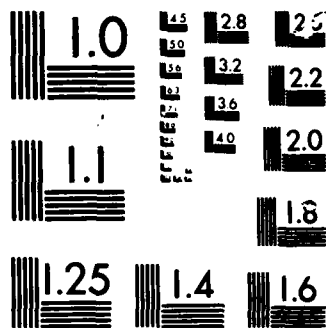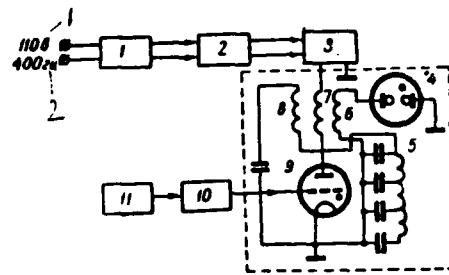
Fig. 105. Diagram of the feeding of a pump lamp: 1- dc supply (convertor); 2- voltage regulator; 3- high-voltage transformer; 4- pulse tube; 5- line for pulse forming; 6- secondary winding; 7- winding for thyratron extinguishing; 8- primary winding; 10- amplifier; 11- generator of trigger pulses.

1- 110 V; 400 Hz

working in pulsed regime. For example, the device for the tracking of airborne targets uses laser based on calcium wolframate with the admixture of neodymium.

The active substance has the form of a bar of length of 50.8 mm and diameter of 6.3 mm. The pumping is done by a tube-like flashlamp. The active substance and the pumping lamp are placed in a cylindrical reflector of the diameter of 50.8 mm, and are cooled by a fan. Temperature of the bar surface does not exceed 130 °C. Frequency of the pulse repetition is 10 Hz, duration of the pulses 35 μsec, power in the pulse more than 1 kw, mean power of the radiation 300 mW, beam width behind the collimating lens 10 mrad, and maximum efficiency coefficient is 0.01 %.

Pumping lamp is feeded by the circuit shown in Fig. 105. Maximum energy necessary for lamp ignition is 30 J. Reliable lamp
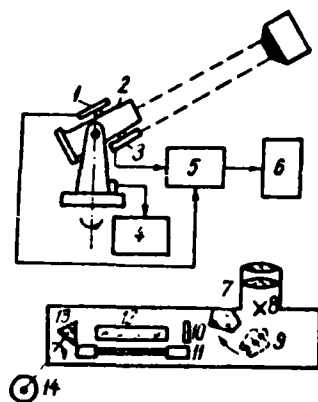
Fig. 106. Diagram of the system for automatic tracking of AES: 1- receiving system; 2- tracing telescope; 3- laser; 4- counter and evaluator; 5- amplifier; 6- indicator; 7- ocular; 8- crosslike grid; 9- prism; 10- semitransparent mirror;11- pumping lamp; 12- ruby crystal; 13- rotating prism (n=12,000 rev/min); 14- motor driving the prism.

ignition and prevention of breakdown at high temperatures and high repetition frequencies are achieved by means of ceramic hydrogen thyratron connected in series with both the power supply and the pumping lamp. The weight of the pumping block is 30 kg.

Pulses reflected by the object are used for distance determination and for forming the difference signals in angular coordinates in two mutually perpendicular planes. Devices intended for this purpose are described in detail in [13]. Difference signals act on servodrives that control the optical elements so that the main optical axis of the system automatically aims in the direction of the tracked object.

A similar system, depicted in Fig. 106 [23], is used for tracking the artificial Earth satellites (AES). Laser 3, irradiating pulses of the duration of several tens of nanoseconds with the repetition frequency of 1 Hz into the direction of AES, is mounted on optical tracing telescope 2. Energy of a pulse is 1 J.

93

There is a mirror corner-like reflector on the AES, that reflects the radiation back at the angle of 10^{-4} rad. The radiation reflected from the satellite is received with an optical system consisting of the objective of the diameter of 470 mm and of the photomultiplier of the dissector type, used in the block of distance measurement and in the target coordinator. Optical system of the transmitting part generates beams with the divergence of 10^{-3} rad.

The system can track an AES both automatically or with the help of an operator, who can trace the AES through the oculars of either the receiver or the transmitter. To this end, the laser must be switched off and a reflecting prism is introduced into the viewing field of the transmitter.

The operating range of the system can be determined by means of the formula

$$D^4 = \frac{16 E_\mu \lambda \tau_a^2 \rho S_{\text{отр}} S_{\text{опт}}}{\pi^3 N h c \theta_{\text{пер}}^2 \theta_{\text{отр}}^2} \text{ км,} \tag{137}$$

where E_μ is the energy of laser radiation, J; λ is the wavelength of the radiation, Å; τ_a is the coefficient of the losses in the atmosphere in one direction; ρ is the reflection coefficient of the corner-like reflector, $\rho=0.5$; $S_{\text{опт}}$ — is the area of the receiving objective, cm²; $\theta_{\text{пер}}$ and $\theta_{\text{отр}}$ — are the angular divergencies of the irradiated and reflected beams, rad; h is Planck's constant, $h=6.62 \times 10^{-34}$ Jsec; N is the minimum number of photons that can be registered against the noise background (determined by the parameters of the photomultiplier). For the
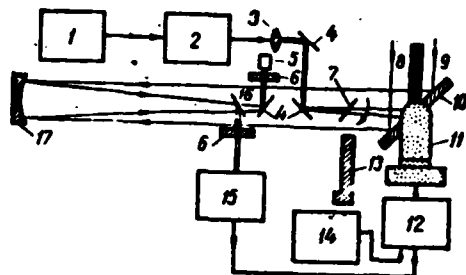
94

Fig. 107. Schematic diagram of a high-precision system of automatic tracking of an object by means of a CW gas laser: 1- He-ne laser; 2- electrooptical modulator; 3- collimating lens; 4- reflecting mirrors; 5- photomultiplier; 6- optical filter; 7- folding mirror of the periscope; 8- modulated laser radiation; 9- signal reflected from the object; 10- turning mirror; 11- Cardan suspension; 12-- servodrive; 13- periscope; 14- system for manual control;- 15- dissector; 16- semitransparent mirror; 17- mirror objective.

chosen parameters of the system, its operating range roughly equals 1500 km.

More recent foreign high-precision systems of automatic tracking are based on the use of gas lasers. Let us look at one of them. The source of the optical radiation in this system (Fig. 107) is He-Ne CW laser 1 operating at the wavelength of 0.6328 μm. The laser radiation goes through optical modulator 2, collimating lens 3, and system 4 of fixed mirrors, and falls on controlled mirror 10 with the diameter of 300 mm, with the help of which it is directed to the target. The same mirror directs the reflected radiation on a parabolic mirror with the diameter

95

of 203 mm and the focal length of 2440 mm, that forms an image of the object on the photocathode of dissector 15.

A semitransparent mirror situated behind the parabolic mirror splits the beam in two. One part of the beam goes through filter 6 with the pass band of 10 Å and falls on photomultiplier 5, that generates the distance signal. The second part arrives through an identical filter into the dissector which consists of a photomultiplier with a semitransparent cathode and electron scanning of the photoelectron beam to determine the angular coordinates of the object in two mutually perpendicular planes. In this way, the position of the image of the object in the plane of the photocathode is investigated in the dissector tube and the difference signals are generated, which are then used for the control of servomechanism of the tracing mirror. The principle of the operation of the electro-optical coordinator with the dissector tube is discussed in [13].

The distance is measured by the relative phase shift of the reflected and irradiated signal. To this end, the laser radiation is modulated according to the sine law by means of an electro-optical modulator. The tone modulation ensures also an additional selectivity, necessary for the selection of the useful signal on the background with a sharp change of the reflection coefficient.

All optical elements of the system are mounted on an optical bench. Here there is also situated the target periscope with a large viewing angle with the help of which the operator manually directs the controlled mirror. When signals reflected from the target appear, the operator switches from manual control to the

automatic tracing.

The controlled mirror is mounted in a cardan suspension the axes of which are driven by dc servomotors. With the axes, there are kinematically connected tachogenerators, which provide a flexible feedback. The axes are fixed in precise bearings. The magnitude of static precision with respect to both axes equals roughly 10μrad.

The transmission coefficient of the optical system taking into account all losses is 0.2. The measured minimum power of the received signal is 8×10^{-10} W. Maximum error of the tracking of an object moving with angular acceleration of 0.6 rad/sec² is roughly equal to 0.30 mrad; for smaller acceleration the error decreases to 0.10 mrad; in the case of the motion without acceleration, but with a sufficient angular velocity, the r.m.s. tracking error equals 0.025 mrad [68].

Let us now discuss a system of automatic tracking distinguished by increased precision. The system consists of two channels of angular tracing of the object, a channel of distance measurement, and a corner-like reflector mounted on the object. Each channel of angular tracking has two axes of rotation: a primary one, characterized by large angular velocity, and secondary one, ensuring a precise automatic tracking in the case of high speeds of the laser beam scanning. The mutual movement of axes is independent, and is summed later on. With the primary axis of the servodrive, an optical system with viewing field of 16 mrad is connected, that uses the reflected laser radiation of wavelength of 0.6328 μm and also its own thermal radiation of the
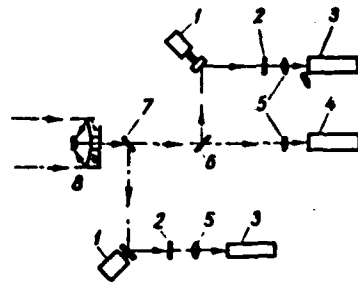
97

Fig. 108. Optical circuit used in the control system of the primary axis of one channel of the automatic tracking of an object: 1- low-power motor with a mirror; 2- modulating disk; 3- photomultiplier of the optical distance finder; 4- condensor lenses; 6- semitransparent mirror; 7- dichroic beam splitter; 8- mirror objectiv.

object in the range of 0.8-2.7 μm. With the primary axis, an optical system with viewing field of 1.5 mrad is connected, using only the reflected laser radiation.

The optical circuit of the control system of the primary axis is schematically depicted in Fig. 108. Its own and the reflected radiation of the object is received by mirror objective 8 of the diameter of 300 mm and directed to dichroic beam splitter 7, transmitting the radiation of wavelength of 0.6328 μm and reflecting the radiation from the range of 0.8-2.7 μm. The radiation 0.8-2.7 μm is modulated with the help of a mirror mounted on the axis of low-power motor 1 (f_m=200 Hz) and of modulating disk 2, and arrives at the photomultiplier of optical coordinator 3 of the target, that generates a signal proportional to the deviation of the object from the viewing line in the given

plane. In a similar way the reflected laser radiation ($\lambda=0.6328$ μm) is used, but only a part of it transverses the semi-transparent mirror into the system of distance measurement, and the rest is received by the photomultiplier of the target coordinator. The control system of the secondary axis operates in the same way.

The system of automatic tracking was modelled on an analog computer taking into account the nonlinearity of the servodrive. To this end, the following maximum values of the parameters of object motion were selected: angular velocity of 1 rad/sec, angular acceleration of 1.5 rad/sec^2, and trajectory curvature of 7.5 rad/sec. The errors for the primary and secondary axes of the servodrives did not exceed 2.3 and 0.275 mrad, respectively [32].

In the system of automatic tracking of a rocket carrier from the moment of launch until the inclined distance of 10 km is reached, one uses scanning of laser beams for the purpose of repeated localization of the rocket, the tracking of which has been lost because of arbitrary reasons, e.g., because of the presence of clouds [85].

With the help of the real-time data on distance, rate of change of distance, and angular coordinates, one can determine the position of the rocket in space with the precision of several centimeters. The system ensures the tracking of the reflector mounted on the rocket with angular precision equal roughly to 1". The instantaneous magnitude of the angular divergence of laser radiation and the viewing field of the photoconvertor amounts to 0.45 mrad ($\approx$1.5'). The repeated localization of the lost object
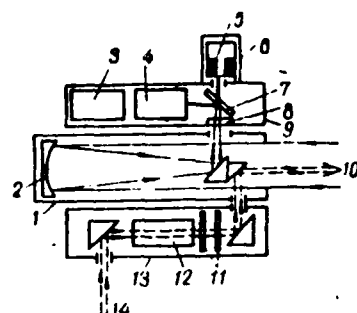
Fig. 109. Diagram of the distribution of electronic and optical elements of the system.

is possible within the angle of $1°x1°$, to which purpose the scanning of a narrow laser beam is performed with the help of an electronic deflection system. The viewing field of the photo-convertor is scanned with the help of a dissector with a semi-transparent photocathode and a secondary electron multiplier (DPFVEU).

Main parameters of the system: laser wavelength: 0.6328 μm; radiative power: 50 mW; effective area of the corner-like reflector: 20 cm^2; maximum velocity during the search: 0.5 deg/sec; maximum expected brightness of the background radiation: 0.2 W/m^2· sr·nm; maximum coefficient of absorption in the atmosphere: 1.2 dB/km; quantum efficiency of DPFVEU: 0.06.

Optical elements of the system are placed in three cylindrical cases (Fig. 109). Laser beam 14 enters lower cylinder 13 through the joint of the optical system with the support, by means of which the spatial position of the optical axis of the receiver-transmitter complex is changed. Then the beam goes through deflection mechanism 12 and optical system 11, which

enables one to set the required beam width and scanning angle. After
being reflected from the rocket, beam 10 is directed to receiving
mirror objective 2, mounted on tube 1. The diameter of the
objective is 150 mm and the focal distance 760 mm. In tube 9
there are situated interferential filter 8, semitransparent
mirror 7, DPFVEU 4 and 6 with deflection coils 5, and electronic
block 3. Deflection coils 5 of the DPFVEU share the workload; one
of them serves for the search and the tracking of the rocket, and
the other for the determination of the distance and velocity with
the help of the modulated signal. Electronic block 3 contains
high-frequency amplifiers, quartz filter, detectors, linear
amplifier, etc.

Deflecting mechanism consists of a series of mirrors, each of
which is mounted on a piezoelectric element working in the regime
of bending oscillations. The mirrors are arranged in such a way
that the total angle of the beam deflection (6 mrad) equals the
sum of the deflection angles of each individual mirror.

Let us investigate the work of the system in the regime of
tracking and search. A difference signal corresponding to the angle
ϕ between the instantaneous position of the optical axis and the
direction to the rocket is generated by the DPFVEU. The process
of forming this signal is shown in Fig. 110. The
difference signal is used in the control system that identifies
the center of the raster with the object within the boundaries of
the viewing field with angular dimensions 1°x1°. If the system
worked in the regime of tracking and the signal disappeared (or
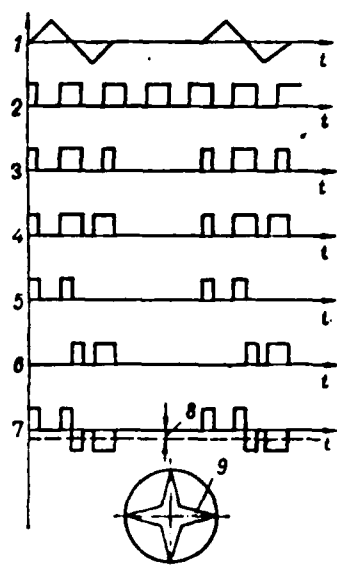its magnitude was less than a threshold value), the system

101

Fig. 110. Forming of the difference signal: 1- signal for crosswise scanning of the square viewing field of the DPFVEU; 2- full signal at the detector output ($\phi=0$); 3- signal in the channel of the spot angle ($\phi=0$); 4- signal in the channel of the spot angle during up and down scanning (the target is shifted downwards with respect to the center); 5 and 6 - selected parts of the signal corresponding to the upper and lower parts of the raster (target shifted downwards); 7- the difference of the selected signals; 8- constant component proportional to the shift of the rocket with respect to the center of the crosswise raster; 9- crosswise raster of the scanning of the DPFVEU viewing field.

would switch in 8 msec from the regime of tracking into the regime of waiting. It lasts 0.39 sec, and if during this time the signal reappears, the system will switch back again into the regime of tracking. If there is no signal, the scanning will start. If the beam hits the rocket and the reflected signal exceeds the set threshold value, scanning will be terminated.

Power F_D of the signal arriving at the photocathode of the DPFVEU, and the signal-to-noise ratio were determined by means of the following formulas [83]:

102

$$F_D = \left(\frac{\pi}{4}\right)^4 \frac{\frac{1}{2} F_r d_{\text{отр}}^4 d_{\text{пр}}^2}{9\lambda^2\theta^2 D^4}\left(\frac{1}{L_n L_{\text{а}} L_{\text{пр}}}\right);$$

$$\frac{\text{signal}}{\text{noise}} = \frac{\left(\frac{m^2}{2}\right)(e\eta/h\nu)^2 F_D^2}{1.33\{2e\,|(e\eta/h\nu)\,F_D|\Delta f + 2e\,|(e\eta/h\nu)\,F_\Phi|\Delta f\}}. \quad (138)$$

where F_r is maximum output power of the laser, W; $d_{\text{отр}}$ — is the
diameter of the reflector on the rocket, m; $d_{\text{пр}}$ — is the diameter
of the mirror objective, m; λ is the wavelength, m; Θ is angular
width of the radiation and of the viewing field of the photo-
convertor, rad; D is the distance to the rocket, m; $L_n, L_{\text{а}}$. and
L_{pr} are the energy losses in the transmitter, the atmosphere, and
the receiver, respectively, dB; m is the coefficient of
modulation; e is the electron charge, C; η is the quantum
efficiency; $h\nu$ is the photon energy, J; Δf is the pass band of
the receiver, Hz; F_Φ is the power of the background radiation
falling on the DPFVEU photocathode, W.
When deriving formulas (138), the following assumptions were made:

1) the width of the beam reflected by the uniformly
illuminated reflector mounted on the rocket is

$$\theta' \approx \frac{3\lambda}{d_{\text{отр}}};$$

2) the constant components of the signal, resulting from the
background radiation, do not pass through the electronic circuits
of the receiver;

3) detector noise and thermal noise in the load can be
neglected;

4) effective power of the carrier in the amplitude modulator

103

is equal to 1/2 F_ν;

5) noise increase caused by dynatron multiplication is assessed by the coefficient of 1.33.

In the end, let us discuss a system intended for the discovery of spaceships and for the determination of the distance between two spaceships for the purpose of their approach and joining [30]. The system consists of two parts, one of which is placed on the approaching ship, and the other on the target ship. On the approaching ship, a semiconductor laser (λ=0.84 μm) for long-range search and long-range distance measurement is situated. The image of the discovered target is projected on an indicator of the dissector type. Beside that, there is a distance finder with a semiconductor laser for the precise distance measurement during the approach of the ships and there is a signal processing block. On the target ship, there is an opto-electronic tracking system with a dissector, optical beacon with a GaAs laser, and a circular grid of corner-like (prismatic) reflectors. The regime of the operation of the system is the following: discovery and the determination of the position of the target ship; long-range tracking and distance measurement; short-range position determination and distance measurement.

Laser beacon 1 serves for the discovery of target ship A (Fig. 111). Laser radiation is received on approaching ship B with the help of objective 2 (input window of 62.5 mm and focal length of 100 mm) and telescopic mirror 3. Viewing field of the optical system equals 10°. After being received by objective 2,
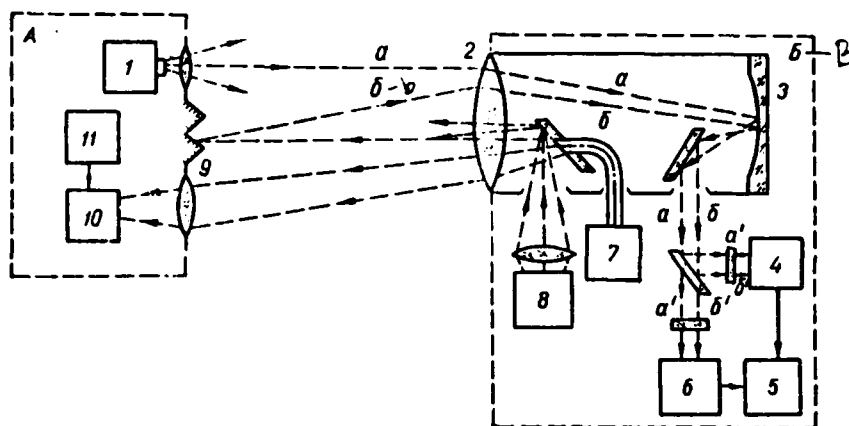
Fig. 111. Diagram of the system mounted on spaceships.

the laser radiation (beam a) is directed by means of a system of
mirrors on the input of image dissector 6. Narrow band (10 Å)
filter performs the spectral selection of radiation. With the
help of dissector 6 and signal processing system 5, the direction
to the discovered ship is   determined.

   After the coordinates of the discovered target ship are
determined, the command to switch off beacon 1 is transmitted. At
that moment, coherent radiator 7 is switched on in the
approaching ship, that operates in the pulsed regime. The
radiation of this source is led through a glass fibre guide and
through an opening in the slanted mirror to objective 2. The
width of the beam on the output of the objective is only 30'.
After the reflection from the elements of reflector grid 9, the
radiation returns to the approaching ship (beam b), and after
passing through the system of mirrors it arrives at the input of
photomultiplier 4 (determination of distance) and the input of
dissector 6 (correction of the target coordinates).

105

According to the signals of the photomultiplier, block 5 evaluates the distance and the velocity within the range of 5-75 m/sec. Part of the radiation from source 7 reaching the target ship falls on dissector 10. In this way it is possible to trace the approaching ship and correct the trajectory of the target ship.

When the distance between the two ships decreases to 3 km, a noncoherent CW source of 5 MHz radiation 8 is switched on in the approaching ship. This radiation goes through elliptic optics, mirror and objective 2 on its way to the target ship in the form of a beam 2.5° wide. After being reflected from the target ship, this radiation arrives at the approaching ship simultaneously on the photomultiplier and the dissector. Block 5 generates information on the distance and determines the mutual speed in the range of 0.3-50 m/sec. The mutual tracking of the ships is performed by means of dissectors 6 and 10 and signal processing systems 5 and 11.

The precision of the measurement of distance is ±0.5 % in the range of 3-14 km and 0.1 % for distances less than 3 km; the precision of the measurement of mutual speed is ±0.3 m/sec and ±0.03 m/sec for large and small distances, respectively; angular coordinates are determined with the precision up to 0.1°, and the angular velocity with the precision up to 0.05 μrad/sec.

28. OPTICAL GYROSCOPES

The function of an optical gyroscope is based on the phenomenon of interference arising when light beams going in opposite directions are summed. This phenomenon was for the first time used by Michelson in the experiments measuring the speed of the rotation of the Earth.

In his first 1904 experiments, Michelson used a system of mirrors situated in the corners of a square (Fig. 112). A beam of parallel rays was directed to semitransparent mirror 1, that splitted the light beam in such way that one beam traversed the system clockwise 2-3-4, and the other, counterclockwise 4-3-2. Both beams were directed through a focusing lens to a screen. When the square rotates about an axis perpendicular to its plane, the beam travelling in the direction of the rotation needs more time to finish the whole path than the beam travelling in the opposite direction. This can be explained by the fact that the mirrors move away from the first beam and approach to the other one. As a consequence of different lengths of path travelled by the two beams, an interferential image can be observed on the screen, and the shift of the interference lines is proportional to the angular velocity of the rotation of the square. Because of the small velocity of the Earth, for a horizontally oriented square with the side of 3 m at the latitude of 40°, this shift amounted only to 10^{-5} of the wavelength. Michelson realized that this effect cannot be registered, in spite of relatively large dimensions of the system (the area of the square formed by the mirror system was 60 m²) he used.

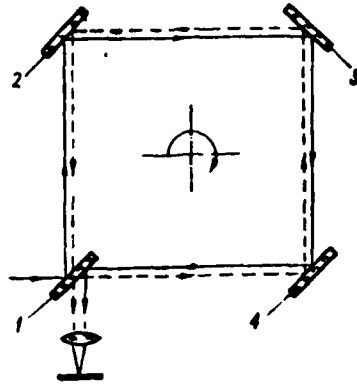A similar experiment was realized by San'yak in 1914

107

Fig. 112. Diagram of the Michelson's experiment for the determination of the speed of Earth rotation.

using four mirrors mounted on a rotating platform. The velocity of the propagation of electromagnetic waves for one direction of beam path equals $c+v$ (where v is the linear velocity of the platform motion), and $c-v$ for the opposite direction. The difference in the beam paths is

$$\Delta L = c\Delta t = c[L/(c-v) - L(c+v)] .$$

Since $c^2 >> v^2$, it is

$$\Delta L = (2v/c)L .$$

The observed shift of the lines corresponded to the calculated magnitude of ΔL.

In 1925, Michelson and Geil repeated this experiment. They used evacuated tubes forming a square with edges 450 m long and showed that the Earth rotation causes a shift of interference lines by a quarter of wavelength. The large dimensions of the apparatus were the main drawback of the practical use of this
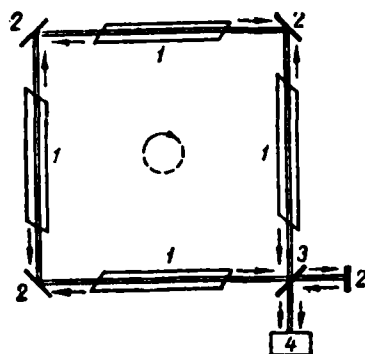
108

Fig. 113. Diagram of an optical quantum gyroscope with four He-Ne lasers.

method for the measurement of angular velocities of moving objects. However, this method was revived with the development of quantum electronics.

The first experimental sample of an optical quantum gyroscope consisted of for He-Ne lasers 1 situated along the edges of a square (Fig. 113). In each of the four corners of the square, there was a mirror 2 the angle of which with respect to the axis of the laser was 45°, so that the beam originating in one generator was reflected by this mirror to the neighboring generator. The lasers irradiated energy from both ends, so that two light beams were moving along the ring-like path in the opposite directions. A part of the energy of both beams passed through the semitransparent mirror 3 and entered the registering device, photomultiplier 4.

As in the linear laser, the generation of light in the ring-like system occurs when the amplification in the active medium exceeds the losses caused by the absorption, diffusion, and

109

$$\sum l_i n_i = N\lambda,$$

where n_i is the refractive index at the i-th segment of the reosonator of length l_i; N is an integer.

If this condition holds, a wave departing from an arbitrary point of the active medium in the resonator returns to this point with phase shift $\phi=2\pi N$, which ensures positive feedback and stable generation.

For simplicity, let us assume that $n_i=n=1$. Then

$$\Sigma\ l_i n_i = N\ ,$$

where L is the perimeter of the resonator.

Putting $\lambda=\frac{v_\phi}{f}$ (v_ϕ – is phase velocity of wave propagation, f frequency), one will obtain

$$f = (N/L)\ c$$

(for a medium with refractive index n=1, $v_f=c=3 \times 10^8$ m/sec).

For $L=L_1$ and $L=L_2$, we have

$$f_1 = \frac{Nc}{L_1} = f\frac{L}{L_1} = f\frac{L}{L-\delta L};$$

$$f_2 = \frac{Nc}{L_2} = f\frac{L}{L_2} = f\frac{L}{L+\delta L};$$

$$F_p = f_1 - f_2 = fL\left(\frac{1}{L-\delta L} - \frac{1}{L+\delta L}\right) = fL\frac{2\delta L}{L^2\left[1-\left(\frac{\delta L}{L}\right)^2\right]}.$$

Substituting the above value for δL and assuming $(\delta L/L)^2 \ll 1$, one obtains

$$F_p = \frac{f}{L}\cdot\frac{4\omega S}{c} = \frac{4\omega S}{L\lambda}. \tag{145}$$

Formula (145) can often be found in the form:

of rotation and lies in the plane of the resonator).

Formulas (140) and (141) give:

$$\frac{c}{v} = 1 + \frac{\omega r}{c} \cdot \frac{1}{\sqrt{1 - \frac{\omega^2 r^2}{c^2}}} r \frac{d\theta}{dl};$$

$$\varepsilon = \frac{\omega r}{c} \cdot \frac{1}{\sqrt{1 - \frac{\omega^2 r^2}{c^2}}} r \frac{d\theta}{dl};$$

$$\delta L_i = \oint \frac{\omega r}{c} \frac{1}{\sqrt{1 - \frac{\omega^2 r^2}{c^2}}} r d\theta. \tag{142}$$

If the speed of rotation is sufficiently small, then $1 - (\omega r/c)^2 \approx 1$, and, therefore,

$$\delta L_i = \oint \frac{\omega r}{c} r d\theta. \tag{143}$$

As can be seen from Fig. 115, product $r^2 d\theta$ approximately equals double the area $2dS$ of triangle OAB, thus,

$$|\delta L_i| = 2\omega S/c , \tag{144}$$

where S is the area of the ring-like resonator.

The sign of δL_i changes when the direction of the gyroscope rotation changes.

Let us now determine the change of the frequency caused by the change of the optical length of the resonator during its rotation. In the stationary regime of the ring-like laser, the length of a closed optical path of radiation propagating in its resonator must be a multiple of wavelength λ:

112

diffraction at the edges of the mirrors. The frequencies of the generated oscillations are determined by several factors, especially by the resonance frequencies of the ring-like optical resonator. If the ring-like resonator rotates about an axis perpendicular to its plane, the paths that two waves travelling in it in opposite directions must traverse to arrive in the point of the active medium where they started will be different. The difference in paths is proportional to the speed of rotation of the resonator. As a consequence of the change of length of closed trajectories of oppositely traveling beams, the frequencies of generated oscillations do change and beats of the difference frequency F_r, proportional to the resonator angular velocity ω. The magnitude of ω can be measured by the output signal of the registering device.

The results of the tests of the device were very satisfactory. For angular velocity of 1 deg/min, the beat frequency was 250 Hz. When angular velocity was changed from 2 to 600 deg/min, beat frequency changed from 500 Hz to 150 kHz approximately linearly (Fig. 114).

Let us derive the formula for difference frequency of beats of two oscillations, traveling in opposite directions along a ring-like resonator rotating with angular velocity ω. To this purpose, let us at first determine the lengths of the trajectories of light beams using the relation

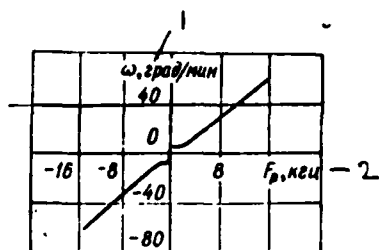$$L_i = \oint (c/v) \, dl \, , \qquad (139)$$

Fig. 114. Dependence of the beat frequency on the angular velocity of the gyroscope (L=4 m; λ=1.15 μm). 1- ω, deg/min; 2-   kHz

Fig. 115. The calculation of the length of trajectories of light beams traveling in opposite directions along a rotating ring-like resonator.

where v is the velocity of light at the given point for the direction of the beam in question; dl is an infinitesimal segment of the resonator perimeter (Fig. 115).

Let us denote $c/v=1+\epsilon$. Then

$$L_i = \oint (1+\epsilon)\, dl = L + \delta L_i \qquad (140)$$

where

$$\delta L_i = \oint \epsilon\, dl .$$

Velocity of light in the moving system is determined by the following formula [41]:

$$v = \frac{c}{1 + \dfrac{\omega r}{c\sqrt{1 - \dfrac{\omega^2 r^2}{c^2}}}\, r\dfrac{d\theta}{dl}}, \qquad (141)$$

where r is the radius vector of a point of the trajectory of the light wave in the resonator (radius vector starts in the center

$$F_p = \frac{4S}{\lambda L} \omega \cos \gamma.$$

(146)

where γ is the angle between vector ω and the normal to the resonator plane.

Coefficient $k = 4S/(\lambda L)$ for the given ring-like laser is a constant quantity, that is why one can write

$$F_p = k\omega \cos \gamma.$$

(147)

When using a square resonator with the side of the square equal to 10 cm, the beat frequency for working wavelength of 0.5 μm is approx. equal to 2×10^5 Hz for angular velocity of the system rotation of 1 deg/sec.

If there is a quadratic photodetector at the output of the system, the signal frequency at its output is equal to the beat frequency. However, measuring the resonance frequency F_p, one can determine only the speed of rotation, but not its direction. To determine the vector of angular velocity, it is necessary to introduce a known frequency shift ΔF, i.e. to shift the origin of the counting of frequency F_p. The initial frequency shift is necessary also for the elimination of the dead region when measuring small angular velocities. This question will be investigated somewhat later; at present let us mention factors that influence the sensitivity and stability of an optical gyroscope.

According to Eg. (145), the sensitivity of an optical

gyroscope is

$$\frac{dF_{\text{г}}}{d\omega} = \frac{4S}{L\lambda} = k.$$

It is directly proportional to the ratio of the resonator area to its perimeter and inversely proportional to the working wavelength. For a triangular resonator with side l, we have:

$$S = \frac{\sqrt{3}}{4} l^2; \quad L = 3l; \quad \frac{S}{L} = \frac{\sqrt{3}}{12} l,$$

i.e., the sensitivity of an optical gyroscope increases with its linear dimensions.

For a triangular He-Ne laser with side l=30 cm, working at wave λ=0.632 x 10^{-6} m, we have

$$k \frac{dF_{\text{г}}}{d\omega} = \frac{\sqrt{3}l}{3\lambda} = \frac{\sqrt{3} \cdot 0.3}{3 \cdot 0.632 \cdot 10^{-6}} \approx 3 \cdot 10^5.$$

The current generated by the photodetector has a nearly sinusoidal form, that is why the value of ω can be obtained in the digital form. To this end, the output signal is cut off and differentiated, and the number of resulting pulses is then counted. The smallest change of frequency measurable by a digital indicator (in the case of counting interval of 1 sec) is $(dF_{\text{r}})_{\min}$ = 1/2 Hz. The change in velocity corresponding to this frequency change amounts to

$$(d\omega)_{\min} = 1/(2k) \ \sec^{-1}.$$

The magnitude of $(d\omega)_{\min}$ represents the theoretical

115

resolution in angular velocity of an gyroscope. For the investigated case, $k=3 \times 10^5$, and, therefore,

$$(d\omega)_{min} = 1/(2 \cdot 3 \cdot 10^5) \approx 1.7 \times 10^{-6} \text{ sec}^{-1} .$$

Measuring continuously the change of phase ψ of the difference signal, one can measure the angle of rotation of the gyroscope from the initial position. Indeed, on the basis of Eq. (147), one can write

$$\Omega_\nu = \frac{d\psi}{dt} = 2\pi F_p = 2\pi k \cos\gamma \frac{d\alpha}{dt},$$

which gives

$$\psi = \psi_0 + 2\pi k \cos\gamma \, (\alpha - \alpha_0).$$

Since the smallest change of phase registered by a digital indicator equals π, the largest measurable angle of rotation (for $\cos\gamma = 1$) is

$$(\alpha - \alpha_0)_{min} = (\psi - \psi_0)_{min}/(2\pi k) = 1/(2k) .$$

Thus, for $k=3 \times 10^5$,

$$(\alpha - \alpha_0)_{min} = 1/(2 \cdot 3 \cdot 10^5) \approx 1.7 \times 10^{-6} \text{ rad} \approx 0.3'' .$$

An arbitrary random change of laser frequency can be the source of a drift of the gyroscope zero as a consequence of the fluctuations in the difference signal phase. An instability of the laser frequency is connected to the oscillations of the properties of the medium filling the optical resonator, and to the changes of the distance between the mirrors. For example, for
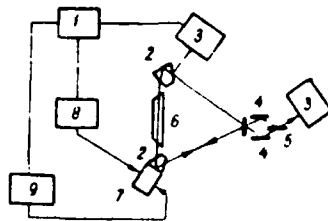
Fig. 116. The diagram of optical quantum gyroscope with an automatic control of resonator length: 1- synchrodetector; 2- prism; 3- photodetector; 4- mirrors; 5- semitransparent mirror; 6- laser; 7- piezoceramics; 8- modulator; 9- servomechanism.

a laser with working wavelength of 1 μm and with a tube 100 mm long, the laser frequency changes by one linewidth, which equals 10 kHz, if the distance between the reflectors changes by 5×10^{-2} Å.

The error arising as a consequence of the change in l can be eliminated by a rigid construction and by thermostating. The frame holding resonator mirrors is made of invar (having temperature coefficient of 2×10^{-6} deg^{-1}) or in the form of a monolithic block of smelted quartz. At present, the principal source of errors of an optical gyroscope seems to be the instability of false zero resulting from anisotropy and also from the phase fluctuations of the difference signal caused by the nonmonochromaticity of the oscillations generated by the laser.

To increase the stability of an optical gyroscope, one uses systems of automatic control of the resonator length. One of such systems is depicted in Fig. 116 [41]. Prism 2 is mounted on a piezoceramics base, therefore, the resonator length can be changed by several wavelengths. The variation of the resonator

117

length generates an error signal, which is used for servo control.

Let us discuss the peculiarities of the construction of modern optical gyroscopes according to the data in foreign literature.

While the first quantum gyroscope had an optical length of 4 m and occupied the area of 9.3 m², newer types of similar devices have total resonator length of approx. 33 cm and occupy an area 75 times smaller. This is because the first quantum gyroscopes used gas lasers with the discharge-tube length of 1 m and diameter of 15 mm. The exploitation of such lasers proved to be difficult because of large length of the tube and the necessity to maintain large degree of parallelism of the reflectors of optical resonators. Later on, these difficulties were partially overcome by the use of nonplanar reflectors, which considerably simplified the adjustment of the device. However, the best results were obtained when using small-size gas lasers having large thermal and mechanical stability. In this case, one can use planparallel reflectors, and have a simple adjustment as well. Such a laser has the form of a quartz rod containing a hollow of the diameter of several millimeters along its whole length. The axis of the hollow is identical with the axis of the rod. Two side canals, ending in cavities containing molybdenum electrodes, are joined with the central hollow.

Modern constructions of quantum gyroscopes use triangular ring-like resonators instead of the quadrangular ones used in the first samples. Such constructions have some advantages. In
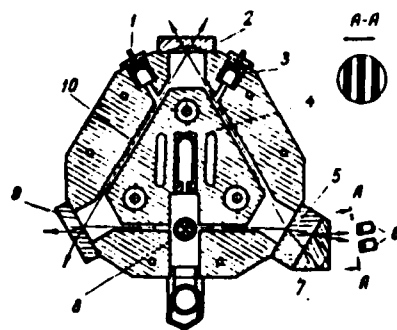
Fig. 117. Construction of an one-axis quantum gyroscope in a monolithic quartz block: 1 and 3 - anodes; 2- spherical mirror; 4- cathode; 5- semitransparent mirror; 6- photomultiplier; 7- prism; 8- diaphragm; 9- mirror; 10- canal with the active medium (l=125 mm).

particular, in the case of an odd number of mirrors, the system has the property of self-adjustment. Besides that, in the case of smaller number of sides, gyroscope tuning becomes easier and energy dissipation smaller.

One of the latest constructions of one-axis quantum gyroscopes, instead of individual tubes and mirrors, uses a block made of high-quality smelted quartz, in which holes and cavities are ground for laser beams, two anodes and cathodes, and for filling the system with a mixture of gases (Fig. 117). Internal cavities are evacuated and filled with a He-Ne mixture under the pressure of 5 mmHg. Between the cathode and the anodes the voltage of 1000 V is applied.

The mirrors are made by means of depositing a large number of thin films of a dielectric on individual pieces of quartz that are then joined to the lateral faces of the block by molecular

119

cohesion. To this end, the surfaces to be joined are polished with the precision of the order of 0.1 μm. One of the three mirrors is spherical. Shifting it, one can adjust the resonater during the assembly of the device.

For the measurement of the frequency differences, the beams are led from the gyroscope in such a way that they are nearly parallel, and they create an interferential image. The direction and the velocity of the gyroscope rotation is determined with the help of two photoelements. If the signals from the photoelements are led to a pulse counter, the device can be used as an integrating gyroscope. According to the foreign data, such gyroscopes retain a linear characteristic for angular velocities up to 1200 deg/sec and even larger. The lower limit is 0.1 deg/h (0.00003 deg/sec). To eliminate the influence of temperature oscillations, a thermostat is used to maintain constant temperature in the quartz block.

The next stage in the development of optical gyroscopes will be the creation of a three-axis gyroscope, containing three planar gyroscopes in a single spherical quartz block. Such a gyroscope could be used, according to the opinion of foreign specialists, in the control systems of rockets, cosmic probes, ships and submarines.

The main advantage of optical quantum gyroscopes in comparison with the classical ones is the absence of any rotating elements. In the electromechanical gyroscopes, a precession of the main axis of the gyroscope with the velocity of 100-500 deg/h arises because of the friction in the pivots of the Cardan

support and imperfect balancing.

In the latest types of gyroscopes with rotors, placed in a liquid, a gas, or an electrostatic or magnetic field, the drift velocity of the main axis can be decreased to 0.01 and even to 0.001 deg/h, however, the construction of such gyroscopes is complicated and their price high. This disadvantage is eliminated in the quantum gyroscopes because their main elements are fixed. At the same time, one can achieve very rigid constructions withstanding accelerations of tens of g.

Dynamical range of measurement of quantum gyroscopes is larger than that of the classical ones. They can measure angular velocities of nearly zero values, with an error less than 0.001 deg/h, and also very large speeds up to 100 rev/sec.

One of the common disadvantages of quantum gyroscopes is the existence of a dead zone caused by the phenomenon of beam capture. In principle, this phenomenon can be explained in the following way. Because of the defects of various elements of the ring-like resonator, part of the energy of the light flux propagating in the given direction interacts with the energy of light flux travelling in the opposite direction. If the gyroscope angular velocity is sufficiently small, then in the course of its further decrease to certain treshold value, called the treshold of blocking, the beats between the waves propagating in opposite directions will suddenly disappear. In the range between zero angular velocity and the treshold of blocking there is a dead zone, which can be several hundred of Hz wide. The blocking treshold decreases with the increase of the area surrounded by

121

the gyroscope beams and the diameter of the beams, and increase proportional to the square of the laser wavelength and to the square root of the dissipation losses.

There are severals methods to eliminate this drawback. One of them is an artificial shift of the frequencies of the two beams, which enables to work sufficiently far from the blocking threshold. An artificial frequency shift, imitating gyroscope rotation, can be created, e.g., with the help of Faraday cells situated in the path of the beam propagation. It was shown in Chapter 2 that in a Faraday cell the refractive index, and consequently also the optical length of the cell, are different for beams propagating in opposite directions.

A disadvantage of this method consists in that an element characterized by relatively large light diffusion is introduced into the gyroscope resonator. Moreover, the shift caused by this element must be maintained with a large precision. However, the results obtained with this method are good; the stability of beat frequency is very satisfactory [41].

Another method of the introduction of artificial shift is the use of a servomotor continuously rotating the quantum gyroscope with a constant speed. This method leads to the increase of the size and the weight of the device.

There is still another method in which the quantum gyroscope is subjected to small oscillations with the frequency of 10-40 Hz. Instead of a constant shift, one gets a continuously changing shift of known amplitude and frequency. During most of an oscillation period, the gyroscope has a fully determined velocity

122

above the blocking treshold. Therefore, very small angular velocities can be measured. Only during two very small time intervals in each oscillation period, the gyroscope angular velocity decreases below the natural blocking treshold. This method does not eliminate completely the main drawback of quantum gyroscopes, but it enable to measure angular velocities less than 0.1 deg/h [41].

29. OPTICAL ALTIMETERS

Range finding laser devices can measure the distance of fixed or moving objects with a high precision. That is why such systems are expediently used for the measurements of the flight altitude of airplanes. According to the opinion of the foreign specialists, the most perspective use of optical altimeters seems to be the measurement of small altitudes because the measurement of such altitudes by means of barometric and radiolocator altimeters is burdened with large errors.

Let us investigate an optical altimeter using a semiconductor laser. Here the airplane altitude is determined, as in radio-altimeters, by the time interval in the course of which the pulse is reflected from the Earth surface and returned to the airplane [34]. Altimeter consists of a transmitter, a receiver, and a indicator. The main element of the transmitter is a semiconductor laser operating at the temperature of 30 °C.

The magnitude of the current passing through the diode (in the pulse) equals 1000 A; length of pulse 30 nsec; repetition
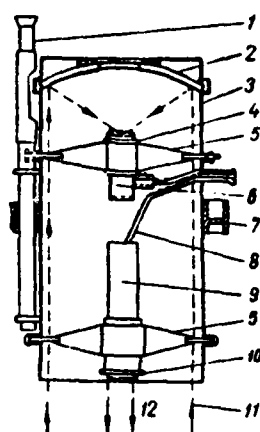
123

Fig. 118. Schematic diagram of the construction of an altimeter with a semiconductor laser: 1- telescope; 2- receiving mirror; 3- case; 4- photodiode; 5- supporting elements; 6- preamplifier; 7- flange; 8- cables; 9- laser and pulse generator; 10- output lense; 11- received beam; 12- transmitted beam.

frequency 15 Hz; power of the pulse leaving the device 10 W; density of radiation 10^5 W/cm^2; angle of beam divergence 20°; working wavelength 0.9 μm; spectral width 50 Å.

The laser is situated in the focal point of a length with the focal distance of 57 mm. Beam divergence when leaving the lense is 0.5°.

The receiver contains a mirror of the diameter of 270 mm and focal length of 120 mm, and a silicon photodiode of the p-i-n type. The mirror projects the image of distant objects on the surface of the photodiode covered with a layer of plastic to decrease the reflection losses. The diameter of the sensitive part of the diode equals 2 mm. Viewing angle of the receiving mirror is 1°. This quantity is increased to make more easier the adjustment of the device.

The main source of noise in the receiving system is the load resistance of the photodiode, and not the background radiation

noise. For the width of the transmission line of 100 MHz, the sensitivity of the system is 0.1 μW, which is larger than the sensitivity that can be achieved with photomultipliers in the conditions of day-light illumination.

As the indicator, an oscilloscope is used. However, the device output can be also converted to digital form, using a counting circuit triggered by pulses from the transmitter output and from the receiver input.

Altitude construction is schematically depicted in Fig. 118. In the upper part of cylindrical case 3 of the diameter of 270 mm, there is receiving mirror 2. Laser and pulse generator 9 are placed in the lower part of the case. Laser focusing is realized by means of the change of the position of the corresponding lens. Photodetector 4 and the cascade of preliminary amplification are situated near the receiving mirror. Telescope 1 serves as the finding device of the altimeter. It was determined experimentally for various types of Earth surface that by means of the described altimeter an altitude up to 300 m can be measured with a precision less than 1,5 m. When the Earth surface is covered by a forest, the reflected signal has the character of a double echo caused by the reflection from the top of trees and from the Earth surface.

30. VELOCIMETERS

Using lasers in Doppler systems for velocity measurements,

one can considerably increase the precision of the velocity measurement. To this end, CW gas lasers are the most suitable ones, because they can generate narrow monochromatic light beams.

When using a velocimeter on a flight machine, the laser beam is directed aslant towards the Earth surface. The receiver is a photoelement, receiving the signal of frequency ν from the laser and the signal reflected from the Earth at the frequency $\nu+\Delta\nu$. Doppler frequency is separated directly at the mixer load. It is determined by the formula

$$\Delta\nu = 2\nu(v/c) \cos\gamma , \qquad (148)$$

where ν is the laser frequency; v is the speed of the flight machine; γ is the angle between the direction of the beam and that of the flight machine.

For v=1000 km/h, λ=1 μm, and γ=85°, one has $\Delta\nu$=50 MHz. In usual Doppler systems working in cm range, this quantity is of the order of 10 kHz.

According to the data from foreign literature [29], the resolution of Doppler navigation systems using He-Ne gas lasers is approximately four times that of conventional systems working in the cm range. The range of measured velocities lies in the range from 0.0003 cm/sec to 8 km/sec.

In a Doppler optical velocimeter of a moving object with UHF modulation, one utilizes the Doppler shift of the UHF signal frequency used for the modulation of the optical carrier. The diagram of such velocimeter is shown in Fig. 119. Modulated
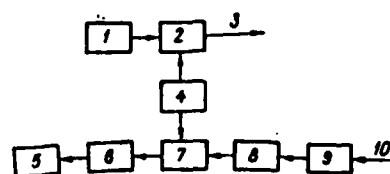
Fig. 119. Schematic diagram of an optical velocimeter with UHF modulation: 1- laser; 2- modulator; 3- transmitted modulated signal; 4- UHF generator; 5- frequency meter; 7- UHF mixer; 8- UHF amplifier; 9- photoconvertor; 10- reflected from the object, modulated signal with the Doppler frequency shift.

signal transmitted in the direction of the object whose velocity is to be measured, can be written in the following way:

$$U_t = U_0 \cos \omega_0 t + \frac{U}{2} \cos(\omega_0 + \omega_m) t + \frac{U}{2} \cos(\omega_0 - \omega_m) t, \quad (149)$$

where ω_0 is the angular velocity of the carrier and ω_m is that of the modulating signal.*

The distance to the object is

$$D(t) = D_0 \pm v(t-t_0) , \quad (150)$$

where D_0 is the distance to the object at time t_0.

Putting $U_0 = U = 1$, one can write the following expression for the signal at the position of the object:

---

* Initial phases are set equal to zero because they have no influence on the results.

127

$$U_t = \cos \omega_0 \left[t - \frac{D(t)}{c} \right] + \frac{1}{2} \cos \left[(\omega_0 + \omega_м)(t - \frac{D(t)}{c}) \right] + {} + \frac{1}{2} \cos \left[(\omega_0 - \omega_м)(t - \frac{D(t)}{c}) \right]. \tag{151}$$

The formula for the signal reflected from the moving object can be writen in the form

$$U_{np} = \cos \omega_0 \left[t - \frac{2D(t)}{c} \right] + \frac{1}{2} \left[\cos (\omega_0 + \omega_м)(t - \frac{2D(t)}{c}) + {} + \cos (\omega_0 - \omega_м)(t - \frac{2D(t)}{c}) \right]. \tag{152}$$

Rearanging individual terms, one obtains

$$U_{np} = \cos \left[\omega_0 \left(1 \pm \frac{2v}{c}\right) t - \frac{2}{c}(D_0 \mp vt_0) \right] + {} + \frac{1}{2} \cos (\omega_0 + \omega_м)\left[\left(1 \pm \frac{2v}{c}\right) t - \frac{2}{c}\left(D_0 \mp vt_0\right) \right] + {} + \frac{1}{2} \cos (\omega_0 - \omega_м)\left[\left(1 \pm \frac{2v}{c}\right) t - \frac{2}{c}(D_0 \mp vt_0) \right]. \tag{153}$$

The carrier, upper, $(\omega_0 + \omega_m)$, and lower, $(\omega_0 - \omega_m)$, frequencies are multiplied by the factor of 2v/c determining the magnitude of the Doppler shift. Angular frequency of the envelope of the signal obtained by detecting and filtering the reflected signal, is

$$\omega_p = \omega_м \left(1 \pm \frac{2v}{c}\right). \tag{154}$$

This frequency is shifted with respect to the initial modulating frequency by a quantity depending on the object velocity. For a modulating frequency corresponding to the ten-cm range, the Doppler shift equals approximately 10 Hz per each 1.87 km/h of velocity.

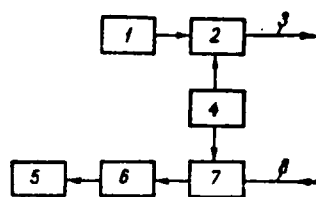The principle of the velocimeter can still be simplified by

128

Fig. 120. Functional diagram of velocimeter with UHF modulation and with dynamic electron multiplier with crossed fields: 1- laser; 2- modulator; 3- irradiated modulated signal; 4- UHF generator; 5- frequency meter; 6- amplifier; 7- dynamic multiplier; 8- reflected from the object, modulated signal with the Doppler frequency shift.
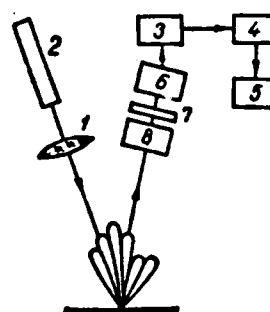
Fig. 121. Block diagram of a diffractional velocimeter: 1- optical system for beam forming; 2- gas laser; 3- LF amplifier; 4- circuit of frequency tracing; 5- voltmeter; 6- photomultiplier; 7- interferential filter; 8- optical grid.

using a dynamical electron multiplier with crossed fields, which has the function of a detector, a mixer, and an amplifier (Fig. 120).

Besides Doppler laser systems of velocity measurement, there are diffractional meters allowing the measurement of the velocity in the direction perpendicular to the laser beam. Their principle is as follows. Let us assume that the laser beam falls on a diffusional reflecting surface. Then the reflected radiation gives a spotty structure consisting of a large number of bright

spots with dark intervals between them. When the reflecting surface is moving with respect to the laser, this structure moves without a considerable distortion of its internal configuration. The velocity of the motion of the difraction pattern is proportional to the velocity of the motion of the reflecting surface.

Schematic diagram of a difractional velocimeter is shown in Fig. 121 [49]. In front of the photoconvertor (photomultiplier 6), diffraction grid 8 with a certain periodicity is placed. When the reflecting surface moves with respect to the laser, the spot traverses individual lines of the grid, which results in a modulated signal on the receiver output. Modulation frequency f_m depends on the grid period t_p and velocity v of the motion of spots with respect to the grid according to the formula

$$f_m = v/t_p .$$

According to the opinion of foreign specialists, the Doppler method has advantages with respect to the diffractional method consisting in the precision and range of operation. Nevertheless, the diffractional method can be used for distances between the laser and reflecting surface on the order of tens of meters and velocities on the order of hundreds of kilometers per hour.

REFERENCES

1. Yu.V. Bayborodin and S.A. Garazha, Electrooptical Effect in the Crystals and its Use in the Construction of Devices,

Moscow, Mashinostroenie, 1967.

2. V.V. Balakov, et al., On Energy Change of Light Pulses, Optiko-Mekhanicheskaya Promyshlennost', No.9, 1966.

3. N.G. Basov, et al., Investigation of the Properties of Injection Lasers in the Range of Wavelengths 0.9-1.1 μm, Zh. Tekh. Fiz, 37, No.2 (1967).

4. L. Bergman, Ultrasound, Izd.Inostr.Lit., 1965.

5. R.A. Balitov, et al., Measurement of the Characteristics of Lasers, Izd. Standartov, 1969.

6. A.P. Zharkov, et al., Laser with Quartz Electrooptical Q-Modulation, Optiko-Mekhanicheskaya Promyshlennost', No.3, 1968.

7. V.I. Zharikov and R.V. Khokhlov, On Light Modulators with Running Wave, Radiotekhnika i Elektronika, 9 (1964).

8. V.Pt. Zuev, Propagation of Laser Radiation, Izv.Vyss.Ucheb.Zav. - Fizika, No. 10, 65 (1967).

9. G. Karsloy, D. Eger, Thermal Conductivity of Solids, Nauka, 1965.

10. G.P. Katys, et al., Modulation and Deflection of Optical Radiation, Nauka, 1967.

11. L.S. Kremenchugskiy and A.F. Mal'nev, Absolute Receiver of Radiation in a Wide Spectral Interval, Pribori i Tekh. Eksperimenta, No. 3 (1968).

12. L.Z. Kriksunov and S.M. Gerasimov, Optical Quantum Generators and their Use, Kiev, Institute of Technical Information, 1965.

13. L.Z. Kriksunov and I.F. Usol'tsev, Infrared Systems for

Discovery, Localization, and Automatic Tracing of Moving Objects, Sovet-skoe Radio, 1968.

14. V.V. Lyubimov and Ye.V. Nilov, Opto-Mechanical Shutter for Q-Modulation of a Laser Resonator, Optiko-Mekhanicheskaya Promyshlennost', No.2, 1967.

15. A.A. Mak, et al., Solid Lasers, Uspekhi Fiz. Nauk, 92, No. 3 (1967).

16. A.L. Mikaelyan, et al., Solid Lasers, Sovet-skoe Radio, 1967.

17. B.N. Morozov, Some Methods for the Measurement of Energy Parameters of High-Power Lasers, Izmeritel'naya Tekhnika, No. 10 (1967).

18. A.P. Pichugin and A.V. Chekan, Methods for Measurement of Frequency Spectrum and Power of Laser Radiation, Zarubezhnaya Radioelektronika, No. 12 (1966).

19. N.N. Sobolev, V.V. Sokovikov, CO_2 Lasers, Uspekhi Fiz. Nauk, 91, No. 3 (1967).

20. V.P. Tychinskiy, High-Power Gas Lasers, Uspekhi Fiz. Nauk, 91, No. 3 (1967).

21. V.N. Chernyshev, et al., Lasers in Communication Systems, Svyaz', 1966.

22. V.A. Shamburov, Optical Indicatrix and Birefringence Surfaces, Kristallografiya, 7 (1962).

23. Experimental Tracing of Earth Artificial Satellites with the Help of Lasers, Zarubezhnaya Radioelektronika, No. 3 (1965).

39. H. Bosc, Utilization of Lasers for the Measurement of Distances, L'Onde Electrique, Vol. 43, No. 437 (1933).

81. G. Tamburelli, Telephone Communications by means of Lasers,

Electronica, No.4 (1966).

(All other references as in the original)

24. A c k e r m a n J. A. Laser energy measuring device. Appl. Optics, 1964, Vol. 3, № 5.
25. A n d e r s o n L. K. Microwave modulation of light. Microwave, 1965, Vol. 4.
26. A n d e r s o n L. K., M c M u r t r y B. J. High-Speed Photodetectors. Proceedings of the IEEE, 1966, Vol. 54, № 10.
27. Applied Phys. Letters. 1963, Vol. 3, № 9, p. 145—148.
28. Applied Optics, 1964, Vol. 3, № 4, p. 507.
29. Awiation Week, 1964, № 20, p. 87.
30. Awiation Week, 1964, June, 1, p. 11.
31. Awiation Week, 1965, № 17, p. 80—85.
32. B a r n a r d T. W., F e n c i l C. R. Digital laser ranging and tracking using a compound axis servomechanism. Applied Optics, 1966, Vol. 5, № 4.
33. B a t e r R. M. Measuring laser output with rat's nest calorimeter. Electronics, 1963, Vol. 36, № 5.
34. B i r b e c k E. E., H a m b l e t o n K. G. A gallium arsenide laser rangefinder used us an aircraft altimeter. J. Scient. Instr., 1965, Vol. 42, № 8.
35. B i r n b a u m G., B i r n b a u m M. Measurment of Laser Energy and Power. Proccedings of the IEEE, 1967, Vol. 55, № 6.
36. B l o e m b e r g e n N., P e r s h a n P. S., W i l c o x L. R. Microwave modulation of Light Ferromagnetic Resonance. Phys. Rev., 1960, Vol. 120.
37. B l o o m A. L. Gas Lasers. Proceedings of the IEEE, 1966, Vol. 54, № 10.
38. B l u m e n t a l R. H. Design of microwave-frequency light modulator. Proc. of the IRE, 1962, Vol. 50, № 4.

40. C a d d e s D. E., M c M u r t r y B. J. Evaluating hight demodulators. Electronics, 1964, № 13.
41. C a t h e r i n J.—M., D e s s u s B. Gyrométres álaser. Electron. industr., 1966, № 99.
42. C h e n o w e t h A. J., G a d d y O. L., H o l s h o u s e r D. F. Carbon Disulfide Traveling —Wave Kerr Cells. Proceedings of the IEEE, 1966, Vol. 54, № 10.
43. C o o k J. J., F l o w e r e s W. L., A r n o l d C. B. Measurment of laser output by light pressure. Proceedings of the IEEE, 1962, Vol. 50, № 7.
44. D a m o n E. K., F l y n n J. T. Liquid calorimeter for high-energy lasers. Appl. Optics, 1963, Vol. 2, № 2.
45. D u l e y W. W. A simple room temperature detector for use with carbon dioxide lasers. J. Scient. Instruments. 1967, Vol. 44, № 8.
46. E i n h o r n R. N. Liquid Lasers for high-power CW operation sought. Electronic Design. 1967, Vol. 15, № 9.
47. E i n h o r n R. N. Picosecond light pulses go begging. Electronic Design, 1967, Vol. 15, № 14.
48. Electronics, 1965, № 18, p. 148—150.
49. Electronic News, 1966, № 444, p. 14.
50. Electronic News, 1966, № 554, p. 36.
51. G o l d s t e i n B. S., D a l r y m p l e G. F. Gallium Arsenide Injection Laser Radar. Proceedings of the IEEE, 1967, Vol. 55, № 2.
52. H a m i l t o n G. W., W o w l e r A. L. The laser rangefinder. Electron and Power, 1966, Vol. 12, Sept.
53. H o d a r a H. Laser Wave Propagation Through the Atmosphere. Proceedings of the IEEE, 1966, Vol. 54, № 3.
54. H o p s o n J. F. Harmonic Structure of modulated Light Beams. IEEE Transaction, 1963, VCS — 11.
55. H u t c h i s o n T. C. and. oth. A precise optical instrumentation radar. IEEE Trans., 1966, AES—2, № 2.
56. J o h n s o n a n d o t h. Measurment of far-infrared laser Power. Rev Scient. Instr., 1969, № 2.
57. K a g a n M. R. and oth. Organic dye lasers Laser Focus, 1968, vol. 4, № 17.
58. K a l i b j i a n R. a n d o t h. Laser Deflection Modulation in a CdS Prism. Proceedings of the IEEE, 1965, Vol. 53, № 5
59. K a m i n o v I. P., T u r n e r E. H. Electrooptic Light Modulators. Proceedings of the IEEE, 1966, Vol. 54, № 10.

60. Kaminov I P., Lik J. Propagation Characteristics of Partially Loaded Two Conductor Transition Line for Broadband Light Modulator. Proc of the IEEE, 1963, Vol. 51, p. 147.
61. Kaminov I. P., Rigrod W. W. Wideband Microwave Light Modulator. Proceedings of the IEEE, 1963, Vol. 51, p. 137.
62. Kerr J. R. A transverse wave phototube for detection of microwave frequency modulated light. IEEE J. Quantum Electronics, 1966, № 2.
63. Kerr J. R. Microwave-Bandwidth Optical Receiver Systems. Proceedings of the IEEE, 1967, Vol. 55, № 10.
64. Kiss Z. J., Pressley R. J. Crystalline Solid Lasers. Proceedings of the IEEE, 1966, Vol. 54, № 10.
65. Leite R. C. C., Porto S. P. S. A simple method for calibration of ruby laser output. Proceedings of the IEEE, 1963, Vol. 51.

66. Li T., Sims S. D. A calorimeter for energy measurments of optical masers. Applied Optics, 1962, Vol. 1, № 3.
67. Lin S. G., Walters W. L. Optical Beam Deflection by Pulsed Temperature Gradients in Bulk GaAs. Proceedings of the IEEE, 1965, Vol. 53, № 5.
68. Lucy R. F., Peters C. J. and oth. Precision laser automatic tracking system. Applied Optics, 1966, Vol. 5, № 4.
69. Miller S. E., Tillotson L. C. Optical Transmission research. Applied Optics, 1966, Vol. 5, № 10.
70. Mitschlecner J. P., Burge D. K., Regelson E. Sea water atenuation measurements with ruby laser. Applied Optics, 1963, № 11.
71. Morton G. A. Infrared detectors. RCA Review, 1965, Vol. XXVI, № 1.
72. Nelson H. High-Power Gaas Laser Diodes Operating at Room Temperature. Proceedings of the IEEE, 1967, Vol. 55, № 8.
73. Proceedings of the IEEE, 1963, Vol.51, № 4, p. 614—615.
74. Proceedings of the IEEE, 1963, Vol. 51, № 1, p. 202—203.
75. Proceedings of the IEEE, 1965. Vol. 53, № 3, p. 436—454.
76. Ross M. Laser Receivers. New York, 1966.
77. Schiel E. J. Photoelectric energy meter for measuring laser output. Proceedings of the IEEE, 1963, Vol. 51, № 2.
78. Snitzer E. Glass Lasers. Proceedings of the IEEE, 1966, Vol. 54, № 10.
79. Sommers X. K. Proceedings of the IEEE, 1963, Vol. 51, p. 261—262.
80. Spencer E. G. and oth. Dielectric Materials for Electrooptic, Elastoptic and Ultrasonic Device Applications. Proceedings of the IEEE, 1967, Vol. 55, № 12.

82. Tischer F. J. Gas-Lens Type Deflection structure for Light Beams. Proceedings of the IEEE, 1967, Vol. 55, № 1.
83. Walsh T. E. Gallium-arsenide electro-optic modulators. RCA Review, 1966, Vol. XXVII, № 3.
84. Whichouse D. R. Understanding CO_2 lasers. Microwaves, 1967, № 7.
85. Weiss P. F., Tohnson R. E. Laser tracking wiht automatic reacquisition capability. Appl. Optics, 1968, Vol. 7, № 6.

END
DTIC

7 - 86